Climatology and Changes of Extratropical Cyclone Activity: Comparison of ERA-40 with NCEP–NCAR Reanalysis for 1958–2001

XIAOLAN L. WANG, VAL R. SWAIL, AND FRANCIS W. ZWIERS

Climate Research Division, Atmospheric Science and Technology Directorate, Environment Canada, Toronto, Ontario, Canada

(Manuscript received 10 February 2005, in final form 25 October 2005)

ABSTRACT

In this study, a cyclone detection/tracking algorithm was used to identify cyclones from two gridded 6-hourly mean sea level pressure datasets: the 40-yr ECMWF Re-Analysis (ERA-40) and the NCEP–NCAR reanalysis (NNR) for 1958–2001. The cyclone activity climatology and changes inferred from the two reanalyses are intercompared. The cyclone climatologies and trends are found to be in reasonably good agreement with each other over northern Europe and eastern North America, while ERA-40 shows systematically stronger cyclone activity over the boreal extratropical oceans than does NNR. However, significant differences between ERA-40 and NNR are seen over the austral extratropics. In particular, ERA-40 shows significantly greater strong-cyclone activity and less weak-cyclone activity over all oceanic areas south of 40°S in all seasons, while it shows significantly stronger cyclone activity over most areas of the austral subtropics in the warm seasons.

The most notable historical trends in cyclone activity are found to be associated with strong-cyclone activity. Over the boreal extratropics, both ERA-40 and NNR show a significant increasing trend in January–March (JFM) strong-cyclone activity over the high-latitude North Atlantic and over the midlatitude North Pacific, with a significant decreasing trend over the midlatitude North Atlantic and a small increasing trend over northern Europe. The JFM changes over the North Atlantic are associated with the mean position of the storm track shifting about 181 km northward. Importantly, there is no evidence of abrupt changes identified for the boreal extratropics, although previous studies have suggested that the upward trend found in the NNR data could be biased high. However, there exist a few abrupt changes over the austral extratropics, which appear to be attributable to the increasing availability of observations assimilated in the reanalyses. After diminishing the effects of these abrupt changes, strong-cyclone activity over the austral circumpolar oceanic region is identified to have an increasing trend in October–December (OND) and July–September (JAS), with a decreasing trend over the 40°–60°S zone in JAS.

1. Introduction

Extratropical cyclone activity plays an important role in the climate system. Cyclones are usually accompanied by adverse weather conditions and also represent a primary mechanism for the poleward transportation of heat and moisture. A systematic change in either the geographical location or the intensity/frequency of cyclone activity will result in substantial precipitation anomalies among other impacts on regional climates. Since the planetary-scale flow is linked to storm tracks (e.g., Cai and Mak 1990), a shift of the storm tracks (i.e., the preferred regions of cyclone activity) will be associated with anomalies in the planetary-scale flow.

There have been many studies using the National Centers for Environmental Prediction–National Center for Atmospheric Research (NCEP–NCAR) reanalysis (NNR) data (Kalnay et al. 1996; Kistler et al. 2001) to assess observed changes of extratropical storm tracks and cyclone activity (e.g., Zhang et al. 2004; Fyfe 2003; Chang and Fu 2002; Gulev et al. 2001; Graham and Diaz 2001; Simmonds and Keay 2000). In particular, Hodges et al. (2003) performed a comprehensive comparison of four reanalysis datasets in terms of storm tracks and tropical easterly waves, using an objective feature tracking method. They have analyzed mean sea level pressure (MSLP) fields, and cyclonic 850-, 500-, and 250-hPa vorticity fields, from the following reanalyses: the 15-yr European Centre for Medium-Range Weather Forecasts (ECMWF) Re-Analysis (ERA-15;

Corresponding author address: Dr. Xiaolan L. Wang, Climate Research Division, Atmospheric Science and Technology Directorate, 4905 Dufferin Street, Toronto ON M3H 5T4, Canada.
E-mail: Xiaolan.Wang@ec.gc.ca

Gibson et al. 1997, plus ECMWF operational analysis for 1994–2001); NNR for 1979–96; NCEP–Department of Energy (DOE) reanalysis (Kanamitsu et al. 1999); and *Goddard Earth Observing Satellite-1* (*GEOS-1*; Schubert et al. 1993). They report that, overall, the four reanalyses correspond very well in the Northern Hemisphere (NH) lower troposphere, although differences in the spatial distribution of the mean intensities show that the ERA-15 is systematically stronger in the main storm-track regions but weaker around major orographic features. Performing a direct comparison of the track ensembles, Hodges et al. (2003) also report that a number of systems with a broad range of intensities compare well among the reanalyses and that a number of small-scale weak systems have no correspondence among the reanalyses or only have correspondence upon relaxing the matching criteria. For the Southern Hemisphere (SH), agreement is found to be generally less consistent in the lower troposphere, with significant differences in both track density and mean intensity, and lower correspondence of cyclonic events. These differences were not all attributable to model resolution. In particular, Hodges et al. (2003) suggested that the subgrid-scale orographic parameterization used in ERA-15 (versus a form of mean or smoothed orography used in the other reanalyses) may be the reason for the differences near major orography features.

However, the comprehensive comparison by Hodges et al. (2003) is limited to the period of 1979–96 (18 yr) and did not include a comparison of historical trends/changes derived from the various reanalyses. Few studies of cyclone activity have been published using the recently completed 40-yr ECMWF Re-Analysis (ERA-40; Uppala et al. 2005; Uppala 2001), and there has not yet been a comparison of ERA-40 with NNR in terms of extratropical cyclone activity. Since both ERA-40 and NNR have data for the 44-yr period from 1958 to 2001, it is possible to make a comparison of the two reanalyses in terms of both the climatology and historical changes in extratropical cyclone activity. The present study aims to make such a comparison.

Cyclones are complex phenomena that may vary in intensity, duration, location, frequency, and vertical structure. Although there is no standard measure of cyclone activity, a number of cyclone activity indices have been developed, including cyclone count statistics (Pettersen 1956; Whitaker and Horn 1984) and eddy variance/covariance statistics (Blackmon 1976; Chang et al. 2002; Hoskins and Hodges 2002; Chang and Fu 2003; Hodges et al. 2003). However, a given index may be closely related to some, but not all, aspects of cyclone activity. Certain indices may better reflect the impacts of cyclones on human society and ecosystems whereas others are better suited to understanding dynamics (Paciorek et al. 2002). For example, cyclone counts have an intuitive match to the phenomena being studied, but they are subject to numerous problems, including arbitrary cutoff values, directional biases (Taylor 1986), difficulties when using a uniform latitude–longitude grid (Hayden 1981), high counts in areas of persistent stationary lows (Lambert 1996), and so on. In particular, a cyclone count index measures neither intensity nor duration of cyclones (Paciorek et al. 2002). To measure the overall cyclone activity, we use a cyclone activity index that is defined as

$$I_y = C_y \overline{L}_y = \sum_{i=1}^{C_y} L_{yi}, \tag{1}$$

where C_y denotes the count of cyclones in a season in year y, and $\overline{L}_y$ denotes the mean intensity of these cyclones, whose intensities are denoted as L_{yi} ($i = 1, 2, \ldots, C_y$). In other words, our cyclone activity index is defined as the seasonal count of cyclones multiplied by their mean intensity (or equivalently, the sum of the intensities of cyclones in a season). However, cyclone occurrence frequency and its distribution, and the life span of cyclone tracks, are also analyzed, in addition to our cyclone activity index. Note that we distinguish a "cyclone" from a "cyclone track" in this study. A cyclone refers to a single low pressure center identified at a specific location (grid point) and time (a terminology commonly used in most of the previous studies); while a cyclone track consists of a cyclone and its trajectory during its lifetime. A cyclone track usually lasts more than one observing interval (6 h in this study) and is present at a series of adjacent grid points in sequence. Therefore, counts of cyclone tracks are usually much smaller than counts of cyclones.

More specifically, we use a cyclone finding and tracking algorithm to identify cyclones and their tracks from 6-hourly MSLP fields of the ERA-40 and NNR reanalyses. The results are compared. Some areas of significant differences, or of significant change over time, are selected for more detailed comparison and analysis.

The datasets used in this study and the analysis procedure will be described in section 2. The cyclone activity climatologies derived from the two reanalyses will be compared in section 3, and the correspondence between individual cyclone tracks in the two reanalyses will be discussed in section 4. Changes in extratropical cyclonic activity over time will be considered in section 5, and concluding remarks will be presented in section 6.

2. Data and procedure

A wide range of fields have been used to study cyclone activity. In general, the use of unfiltered MSLP

TABLE 1. Summary of the ERA-40 and NNR assimilation systems, models, and the assimilated observations/data. Abbreviations and acronyms not already defined in text are as follows: National Environmental Satellite, Data, and Information Service (NESDIS); Television Infrared Observation Satellite (TIROS); TIROS Operational Vertical Sounder (TOVS); Advanced TOVS (ATOVS); High-Resolution Infrared Spectrometer (HIRS); Microwave Sounding Unit (MSU); Advanced MSU (AMSU); Stratospheric Sounding Unit (SSU); Vertical Temperature Profile Radiometer (VTPR); European Space Agency/European Remote Sensing Satellite (ESA/ERS); Scanning Multichannel Microwave Radiometer (SMMR); Geostationary Meteorological Satellite (GMS); Pseudo Surface Pressure Observations produced by Australia (PAOBs); the First Global Atmospheric Research Program (GARP) Global Experiment (FGGE); Tropical Ocean and Global Atmosphere Coupled Ocean–Atmosphere Response Experiment (TOGA COARE); the Alpine Experiment (APLEX); GARP Atlantic Tropical Experiment (GATE); Total Ozone Mapping Spectrometer (TOMS); Solar Backscatter Ultraviolet (SBUV); Global Sea Ice and SST data (GISST); U.K. Met Office (UKMO); and Synoptics (SYNOP).

	ERA-40 (Uppala et al. 2005; Uppala 2001)	NNR (Kalnay et al. 1996; Kistler et al. 2001)
Period (yr)	1958–2001 (44)	1958–2001 (44)
Assimilation	Updated 3DVAR	3DVAR
Model	Spectral model	Spectral model
Horizontal resolution	Triangular truncation of 159 waves (T159)	Triangular truncation of 62 waves (T62)
Vertical levels	60 (hybrid)	28 (sigma)
Satellite	NOAA TOVS, HIRS, MSU, and SSU, VTPR, and AMSU-A (direct radiance assimilation), NOAA ATOVS, ESA/ERS, SMMR, SSM/I, GMS data, Reprocessed Meteosat	NESDIS TOVS (HIRS, MSU, and SSU), NOAA VTPR and HIRS (for SH)
	Cloud winds	Cloud winds
Upper-air data	Radiosondes, dropsondes, pibals, aircraft, profilers	Radiosondes, dropsondes, pibals, aircraft
Surface data	SYNOP (stations), buoys, ship reports (land: pressure, temperature, humidity, snow depth; ocean: pressure, temperature, humidity, wind)	stations, buoys, oceanic reports (land: pressure; ocean: pressure, temperature, humidity, wind)
Specials	PAOBs, FGGE, TOGA COARE, ALPEX, GATE, Canadian snow depth, TOMS and SBUV ozone retrievals	PAOBs, FGGE, TOGA COARE
Boundary	HADISST1 dataset for 1957–November 1998, NOAA/NCEP 2DVAR dataset for December 1998–June 2001	Reynolds SST for 1982 on and UKMO GISST for earlier periods, ECMWF sea ice (and maybe others), NESDIS snow
Orography	Mean orography and parametric subgrid	Mean orography

and 850- or 500-hPa geopotential height fields emphasizes the large spatial-scale features, while the use of cyclonic vorticity fields (at 850-, 500-, or 250-hPa level) tends to identify smaller spatial-scale features (Hoskins and Hodges 2002). A drawback of using unfiltered MSLP or geopotential heights fields is that they are strongly influenced by large spatial scale (such as Icelandic low) and strong background flows (e.g., Hoskins and Hodges 2002). Many researchers have tried to address this problem by removing an estimate of the background flow (e.g., Hoskins and Hodges 2002; Anderson et al. 2003; Hodges et al. 2003), while others have used vorticity fields because these fields do not depend as strongly on the background flow (although they have other problems; cf. Hoskins and Hodges 2002). Anderson et al. (2003) present a detailed study on the sensitivity of feature-based analysis methods of storm tracks to the form of background field removal.

We use MSLP fields in this study in order to focus on the large-scale features of cyclone activity. However, as noted, results may be influenced by the background flow, and may also be biased toward the slower-moving systems. Also, MSLP is an extrapolated field and may be sensitive to how the extrapolation is performed and the representation of the orography in the model (Hoskins and Hodges 2002). To alleviate/avoid these problems, we use the local Laplacian of pressure to measure cyclone intensity and focus mainly on strong cyclones, and we exclude elevated areas (i.e., areas of elevation $\geq$1000 m) when discussing the results (here we use a global elevation dataset on a 2°-by-2° latitude–longitude grid to do the mask).

Global 6-hourly MSLP from ERA-40 and NNR for the period 1958–2001 were used in this study. Table 1 briefly compares the two reanalyses in terms of data assimilation systems, models, and the assimilated observations/data. NNR is a first-generation reanalysis from 1948, which is being continued in close to real time (Kalnay et al. 1996; Kistler et al. 2001). It was based on the NCEP global spectral model with 28 vertical "sigma" levels and a triangular truncation of 62 waves (T62). ERA-40 is a new, second-generation reanalysis that uses an improved data assimilation system, a T159 model, and more observational data than previous reanalyses (Table 1; Uppala et al. 2005).

Despite the differences in model resolution, both

ERA-40 and NNR datasets that were used in this study are available on a 2.5 × 2.5 latitude–longitude global grid. These datasets were interpolated to a 250 × 250 km version of the National Snow and Ice Data Center (NSIDC) Equal Area Special Sensor Microwave Imager (SSM/I) Earth Grid (EASE-Grid; Armstrong and Brodzik 1995) over the Northern and Southern Hemispheres, separately, prior to the identification of cyclones. This processing step is necessary for compatibility with the search logic for identifying cyclones.

The cyclone identification/tracking algorithm used in this study was originally developed by Serreze (1995; see also Serreze et al. 1997) and was used by the National Oceanic and Atmospheric Administration–Cooperative Institute for Research in Environmental Sciences (NOAA–CIRES) Climate Diagnostics Center (CDC) to diagnose storm tracks from current 6-hourly NNR data for up to May 2004. This is an automatic cyclone tracking algorithm that is similar to the scheme originally developed by Murray and Simmonds (1991) and used extensively to analyze Southern Hemisphere cyclone behavior (e.g., Simmonds and Murray 1999; Simmonds et al. 1999; Simmonds and Keay 2000; Sinclair 1997, 1994).

The algorithm used here consists of two components: cyclone detection from a series of 6-hourly MSLP maps and system tracking. The cyclone detection algorithm involves identification of the grid point, or adjacent grid points, with minimum pressure value over a 7 × 7 array of grid points, where the minimum pressure is at least a detection threshold lower than the surrounding grid-point values. When duplicate centers (adjacent grid points with identical pressure values) are found, the cyclone center is defined as the grid point of the largest (most positive) local Laplacian of pressure. The cyclone tracking algorithm uses a "nearest neighbor" analysis of the positions of systems between time steps with a maximum distance threshold between candidate pairings and further checks based on distance moved in the north/south and west directions and pressure tendency. In this study, we used a maximum distance threshold of 800 km and a detection threshold of 1 hPa, which are values used by NOAA–CIRES CDC for deriving its NNR cyclone database. This distance threshold allows a cyclone to traverse, for example, a maximum of one grid point in the north–south direction and three grid points in the east–west direction within 6 h. Such a distance (the equivalent of 133 km h^{-1}) seems "too fast," but allows "center jumps" (i.e., fast-moving centers that travel more than one grid point within 6 h) to be tracked. A large distance threshold is also necessary when one only has data at specific grid points because this implies that cyclone movement must be resolved into one of only a finite number of possible distances. Individual 6-hourly movements may therefore appear to be unphysically large, but average speeds over the life of a cyclone should be well represented.

We ran the algorithm on the ERA-40 MSLP dataset to obtain an ERA-40 cyclone database, while the NNR cyclone database was downloaded from the NOAA–CIRES CDC (Boulder, Colorado) Web site (http://www.cdc.noaa.gov/map/clim/st_data.html). The "detected" cyclones were classified into two intensity categories (weak and strong) according to whether or not their intensity (i.e., local Laplacian of pressure) is below 15×10^{-5} hPa km^{-2}. A local Laplacian of pressure of 15×10^{-5} hPa km^{-2} roughly corresponds to a geostrophic vorticity of 1.2×10^{-4} s^{-1} (at 45°N).

Our analysis of these datasets was performed in a number of stages. First, the two-sample two-sided Student's t test for the case of unknown (and maybe unequal) variances (see section 6.6.5 of von Storch and Zwiers 1999) was used to determine the statistical significance of changes in seasonal cyclone statistics (counts/intensity/index) at each grid point, or in the areal mean life span of cyclone tracks (also called "cyclone duration" in Zhang et al. 2004), between two periods of equal length (e.g., 1958–77 and 1982–2001). The analyses were carried out for each season separately, and in each season, for all cyclones together and separately for the strong and weak cyclones. Serial correlation is not a notable problem in this case because consecutive data points in the time series are separated by one year. Note that it is possible in the above counting procedure for a quasi-stationary or slow-moving cyclone to be enumerated many times, or for a fast-moving cyclone to traverse a grid box without being enumerated. However, the resulting over- or undercounting was proved not to be a problem because the results are corroborated by investigating changes in counts of cyclone tracks.

Data for the Southern Hemisphere very likely have temporal discontinuities that arise from the increasing availability of observations assimilated in the reanalyses (cf. Tables 1–2 and Fig. 1 of Uppala et al. 2005; Chang 2005; Trenberth et al. 2005; Bengtsson et al. 2004). To assess the data homogeneity and to obtain a more realistic estimate of trend in cyclone activity over the Southern Hemisphere, a two- or multiphase regression model–based data homogenization technique (see the appendix and references therein) was also applied in this study.

The analyses are carried out for each season, separately, with the four seasons being defined as January–

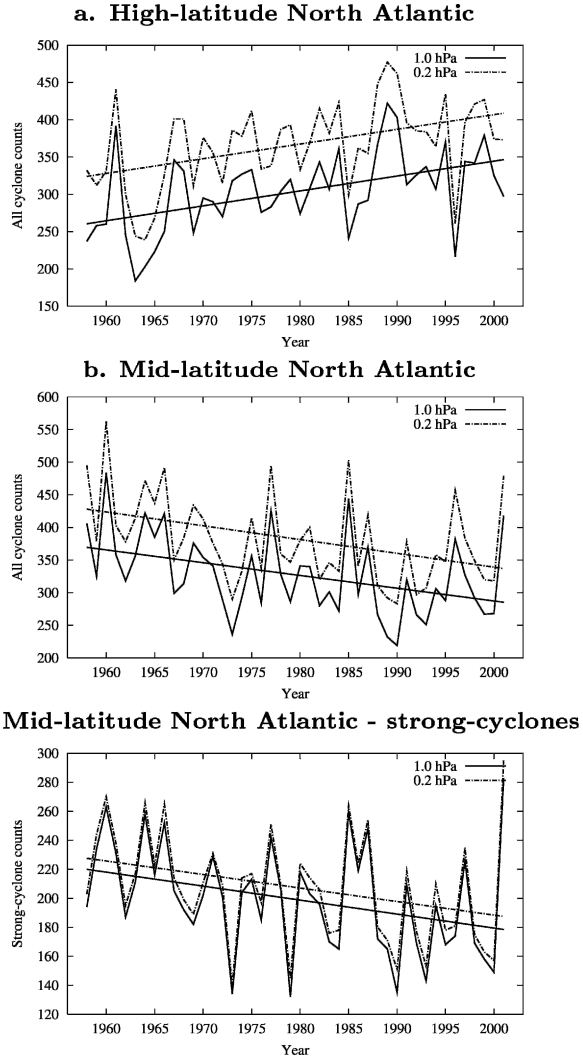

FIG. 1. Time series of counts of winter (JFM) cyclones over (a) the high-latitude North Atlantic (55°–70°N, 45°W–15°E) and (b) the midlatitude North Atlantic (45°–55°N, 75°–10°W), as identified from ERA-40 using detection thresholds of 1.0 and 0.2 hPa (c) The same as (b), but for the counts of winter strong cyclones.

March (JFM), April–June (AMJ), July–September (JAS), and October–December (OND).

The sensitivity of our results to the choice of detection threshold in the cyclone finding scheme was investigated by systematically varying the threshold from 1.0 to 0.2 hPa (the smallest value possible). As a result, we found that there are little differences in the variability and trend of cyclone activity over the 44-yr period, although the number of cyclones (especially weak cyclones) identified increases systematically as the detection threshold decreases from 1.0 to 0.2 hPa (cf. Fig. 1). Since the objectives of the present study are to compare ERA-40 with NNR and to assess historical changes of cyclone activity, with focus mainly on strong-cyclone activity, the parameter choice is unlikely to have significant effects on the results, as long as the same algorithm with the same values of parameters is applied to both ERA-40 and NNR datasets.

3. Cyclone activity climatology—ERA-40 versus NNR

In this section, ERA-40 is compared with NNR in terms of seasonal cyclone activity climatology. The term "significant difference/change" is used here (and throughout this paper) to indicate differences/changes of at least 5% significance (i.e., $p \geq 0.95$; results of two-sided Student's t tests at the 2.5% significance level in each tail). To recap, strong cyclones are cyclones with intensity of 15×10^{-5} hPa km^{-2} or greater.

In terms of the 44-yr mean cyclone activity over the boreal extratropics, generally, ERA-40 shows greater strong-cyclone activity over the oceans than does NNR, especially over the western North Pacific and the Arctic; but there is little significant difference between the two reanalyses over northern Europe, eastern North America, and most areas of the boreal oceans (cf. Fig. 2; AMJ and OND are not shown here, but AMJ is similar to JAS, and OND to JFM). However, ERA-40 shows generally less weak-cyclone activity than does NNR (cf. Fig. 2c), especially over the Canadian Arctic in the cold seasons (OND and JFM; not shown). Some significant differences in weak-cyclone activity are also seen over Siberia and the north shore region of the Mediterranean, and over the leeside of the Rocky Mountains and Greenland in all seasons (cf. Fig. 2c). In particular, ERA-40 shows significantly weaker cyclone activity over the leeside of the Rocky Mountains (cf. Fig. 2c). This is consistent with the findings of Hodges et al. (2003), who report that the ERA-15 cyclone activity is systematically weaker around major orographic features, which may be attributable to the subgrid-scale orographic parameterization used in ECMWF reanalysis (versus a form of mean orography).

To perform a more detailed comparison and analyses, we selected several areas of significant differences between ERA-40 and NNR (and/or of significant changes over time). Any elevated area was excluded from these selected areas, as shown in Fig. 3. We derived the distribution of areal mean seasonal cyclone counts over its intensity for the selected areas and compared the two reanalyses in terms of the cyclone frequency distribution in each season. We also derived time series of areal mean seasonal strong-cyclone activity index (and count) from the ERA-40 or NNR data over these selected areas. The main results are discussed below.

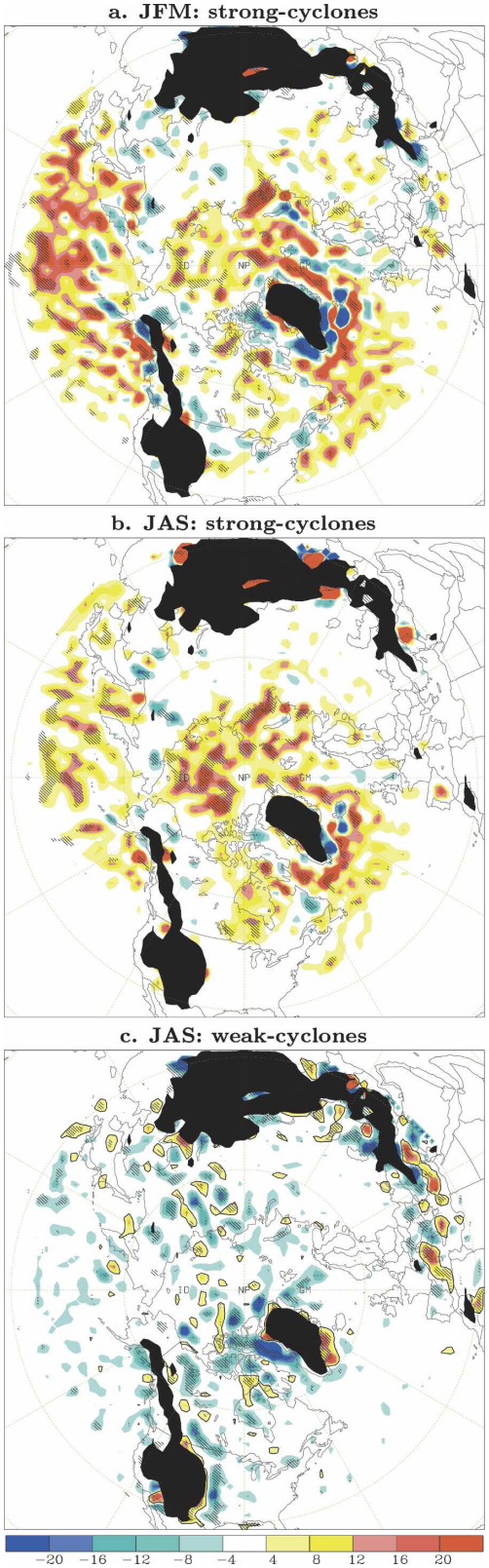

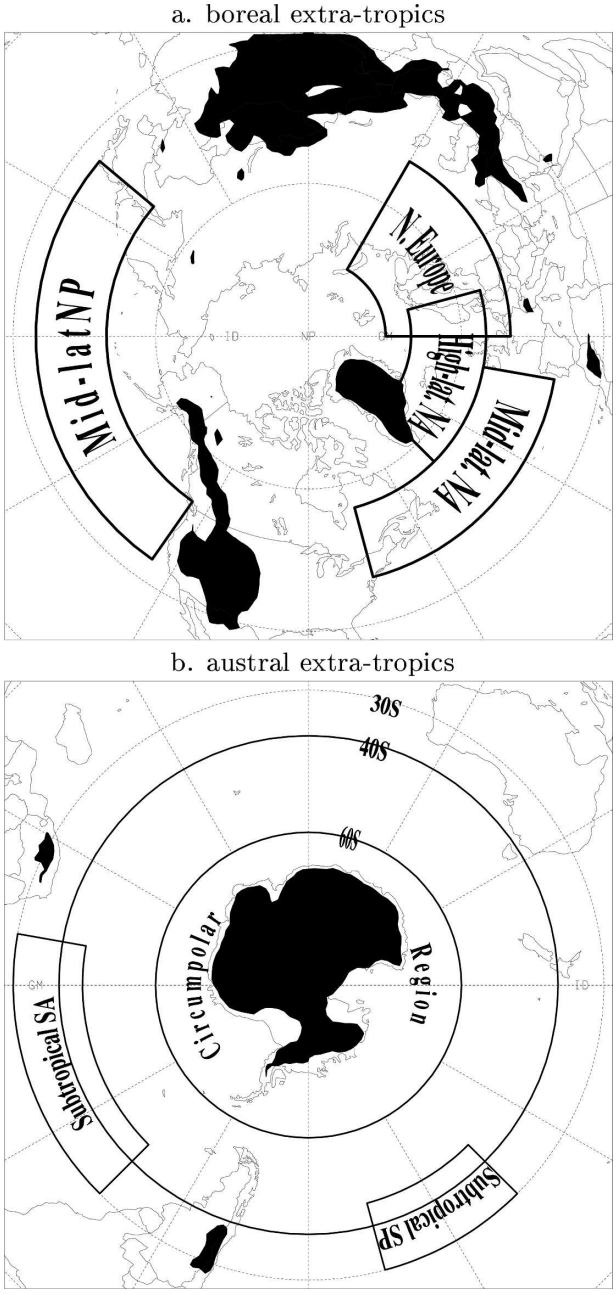

FIG. 3. Selected regions for performing more detailed comparison and analysis. Note that the elevated areas (i.e., black-shaded areas) were excluded from the selected regions: (a) boreal extra-tropics and (b) austral extratropics.

←

FIG. 2. Differences between ERA-40 and NNR 44-yr mean activity index of (a) JFM strong cyclones; (b) JAS strong cyclones; and (c) JAS weak cyclones (ERA-40 minus NNR; unit: 10^{-5} hPa km^{-2}). Red (blue) shadings indicate positive (negative) differences. Hatching indicates regions where the difference is of at least 5% significance (two-sided Student's t tests at 2.5% significance level). Black-shaded areas are elevated areas (with elevation ≥1000 m).

In terms of cyclone frequency distribution, ERA-40 and NNR agree reasonably well with each other over the high- and midlatitude North Atlantic (NA) and over the midlatitude North Pacific (NP). Also, there are only small differences between the early and later decades (i.e., 1958–77 and 1982–2001) in these regions. However, ERA-40 shows slightly fewer moderately strong cyclones (intensity: 15–30 units) with a slightly higher number of intense cyclones (intensity >30 units) over the high-latitude NA in all seasons except OND (cf. Fig. 4a). The effect of fewer moderately strong cyclones is greatly canceled out by the effect of more intense cyclones, so that there is little difference between the two reanalyses for this region in terms of the strong-cyclone activity index (cf. Fig. 5a). ERA-40 also shows slightly higher numbers of strong cyclones and fewer weak cyclones over both the midlatitude NA and the midlatitude NP in all four seasons, with slightly larger differences over the midlatitude NP (cf. Fig. 4b).

In terms of the time series of areal mean seasonal strong-cyclone activity, as shown in Fig. 5, there is reasonably good agreement between the two reanalyses over the high-latitude NA and northern Europe over the entire reanalysis period (except the first decade for northern Europe), while ERA-40 shows systematically greater strong-cyclone activity over the midlatitudes of the boreal oceans than does NNR (especially over the midlatitude NP). Note that, in terms of variability and trends, time series of the areal mean seasonal counts of strong cyclones (not shown) are almost identical to those shown in Fig. 5. So, similar differences exist in terms of seasonal strong-cyclone counts.

Over the austral extratropics, as shown in Fig. 6, significant differences between ERA-40 and NNR are much more extensive, showing more organized patterns of difference than those over the boreal extratropics. ERA-40 shows significantly greater strong-cyclone activity and less weak-cyclone activity over most areas of the austral extratropical oceans than does NNR in all seasons, while it shows stronger weak-cyclone activity over the austral subtropical (30°–40°S) oceans in OND and JFM (cf. Fig. 6 for the strong-cyclone activity; differences in weak-cyclone activity are not shown). The latter difference is more extensively significant in terms of the intensity than the count (not shown). ERA-40 only shows weaker strong-cyclone activity over a narrow zone around 65°S of the South Pacific (SP) in JAS (cf. Fig. 6b), which is more apparent in terms of the count than the intensity (not shown). In comparison with the other seasons, the differences between the two reanalyses for JAS are slightly less extensive for strong-cyclone activity (cf. Figs. 6a–b) but more extensive for weak-cyclone activity (not shown).

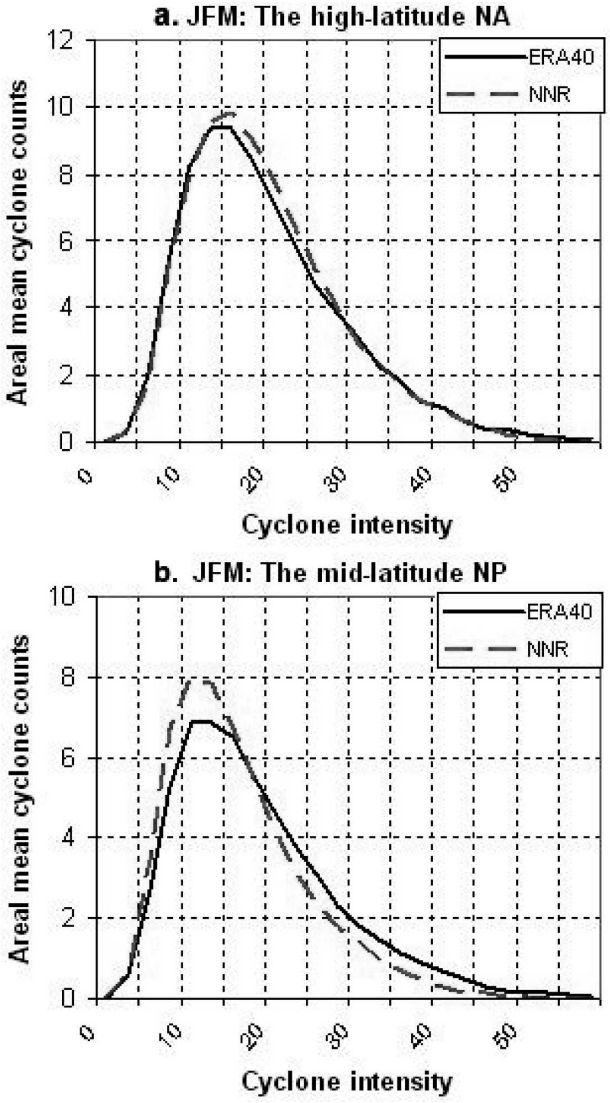

FIG. 4. Distributions of areal mean JFM cyclone counts vs cyclone intensity for (a) the high-latitude North Atlantic and (b) the midlatitude North Pacific. The unit of cyclone intensity is 10^{-5} hPa km^{-2}. ERA-40 shown by solid curve and NNR by dashed curve.

To check whether or not these patterns of difference originate with the introduction of satellite data in 1979, we also performed the comparison between the two reanalyses for the periods 1958–77 and 1982–2001 separately. We found that the patterns of difference have substantial differences between the two 20-yr periods. In OND and JFM, more extensively significant differences between the two reanalyses are seen over the subtropical South Atlantic (SA) in 1958–77, but over the middle- to high-latitude South Pacific in 1982–2001 (cf. Figs. 6c–d). In AMJ and JAS, significant differences

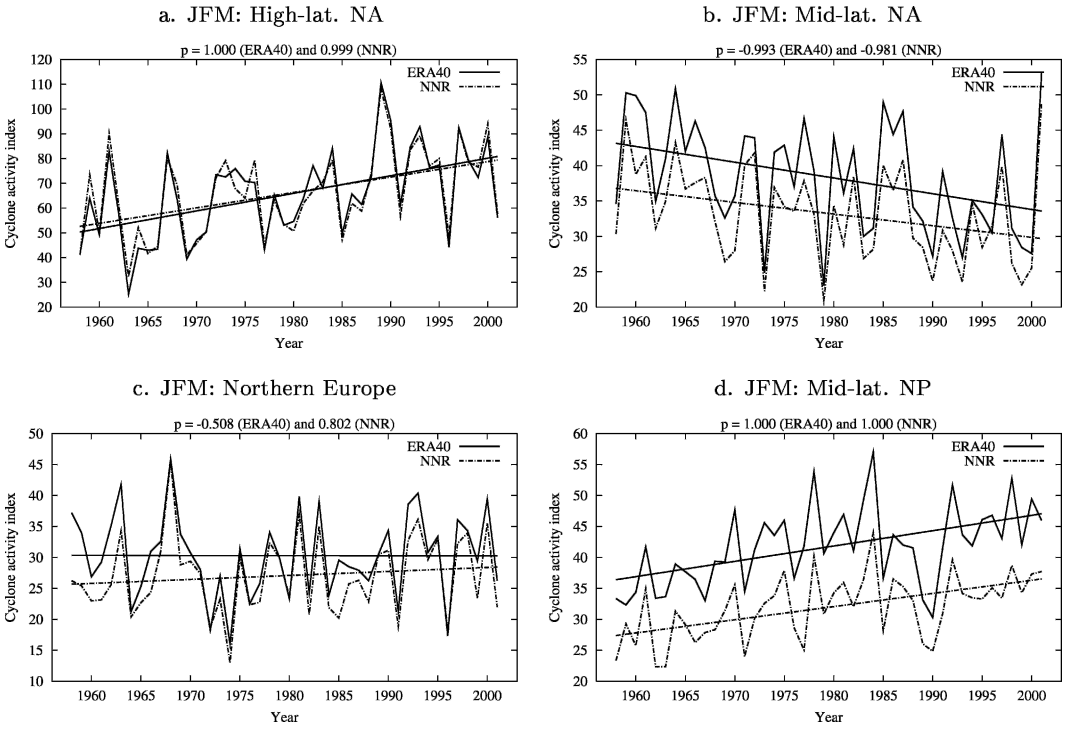

FIG. 5. Time series of areal mean seasonal (JFM) strong-cyclone activity index derived from ERA-40 (solid line) and NNR data (dashed line) for the selected areas in the boreal extratropics (see Fig. 3a for their boundaries): (a) high-latitude and (b) midlatitude North Atlantic, (c) northern Europe, and (d) high-latitude North Pacific. The p values (significance $1 - p$) of trends (straight lines) are also shown on the top of the plots. A negative (positive) p value means a negative (positive) trend.

are much more extensive in the early than the recent decades, especially over the subtropical SA (and subtropical SP in AMJ; not shown). In general, the differences are more extensively significant over the 30°–60°S zone in the early than in the recent decades (Figs. 6c–d).

Generally, ERA-40 shows many more strong cyclones and fewer weak cyclones over the austral extratropics than does NNR in all seasons in both periods 1958–77 and 1982–2001 (cf. Fig. 7). In the 40°–60°S zone, larger differences between ERA-40 and NNR are seen in 1958–77 than in 1982–2001, especially for cyclones of median intensity (cf. Figs. 7a–b; other seasons are similar and hence not shown). For JAS cyclones in the austral circumpolar region (i.e., the region south of 60°S, excluding the elevated Antarctic areas), however, larger differences are seen in 1982–2001 than in 1958–77 (cf. Figs. 7c–d). While this is also true for the JFM strong cyclones in this region, there exist larger differences for the JFM cyclones of moderate intensity in 1958–77 than in 1982–2001 (not shown). The differences between the two periods will be discussed later in section 5.

As shown in Fig. 8, there are large differences between the two reanalyses throughout the 44-yr period over the entire austral extratropics. ERA-40 shows much greater strong-cyclone activity than does NNR in all seasons, especially in the 40°–60°S zone. In the austral circumpolar region, the differences are generally much larger in the recent than in the early decades (except in AMJ; cf. Figs. 8a–d). Over the subtropical South Atlantic, however, much larger differences are seen in the early than in the recent decades in all seasons (cf. Figs. 8i–j). This is also the case for the subtropical South Pacific, especially in the OND and AMJ seasons (not shown).

In particular, there exist abrupt changes (mean shifts) in most of the time series shown in Fig. 8. These are most likely a manifest of the increasing data availability during the reanalysis period, because the years at which these abrupt changes occur coincide well with the years of known increases in the amount of observation data assimilated in the reanalyses (e.g., 1967, 1973, 1979, 1987, and 1992 for ERA-40; cf. Tables 1–2 and Fig. 1 of Uppala et al. 2005). The abrupt changes certainly contribute to the large differences between the two reanalyses in the early decades, especially over the subtropical South Atlantic (cf. Figs. 7c and 8i–j).

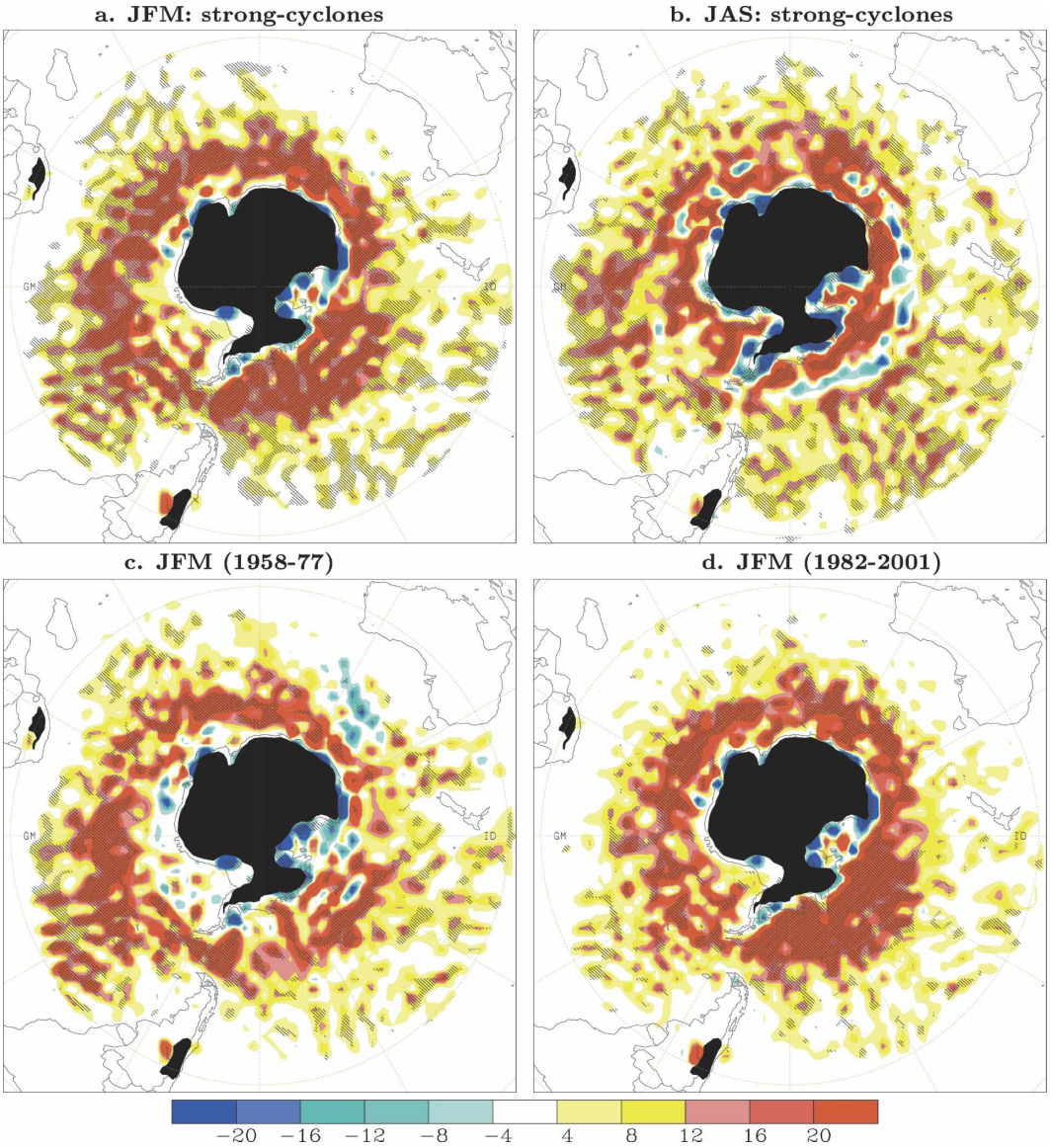

FIG. 6. (a), (b) Same as in Fig. 2, but for the austral extratropical cyclone activity. (c), (d) Same as in (a), but for the comparisons for periods 1958–77 and 1982–2001, respectively.

Trenberth et al. (2005) have attempted to adjust for such spurious variations in the Southern Hemisphere between 1978 and 1979, which was found here to be the biggest problem but not the only problem. Our attempt to diminish the effects of these abrupt changes on trend estimates is described later in section 5b (and in the appendix).

4. Correspondence between individual cyclone tracks

To investigate the correspondence between individual cyclone tracks in the two reanalyses, a comparison in both space and time was performed of the individual members of the ERA-40 and NNR track ensembles (i.e., the "direct comparison of track ensembles" in Hodges et al. 2003). Each cyclone track in the ERA-40 ensemble is compared with those in the NNR ensemble by first finding the tracks in the NNR ensemble that overlap in time with the track in the ERA-40 ensemble. If the number of points that overlap is greater than or equal to 60% of the mean number of points in the two tracks, this is considered a possible good match in time. For the tracks that satisfy the constraint in time, the mean separation on the unit sphere is computed from those points that overlap in time using the geo-

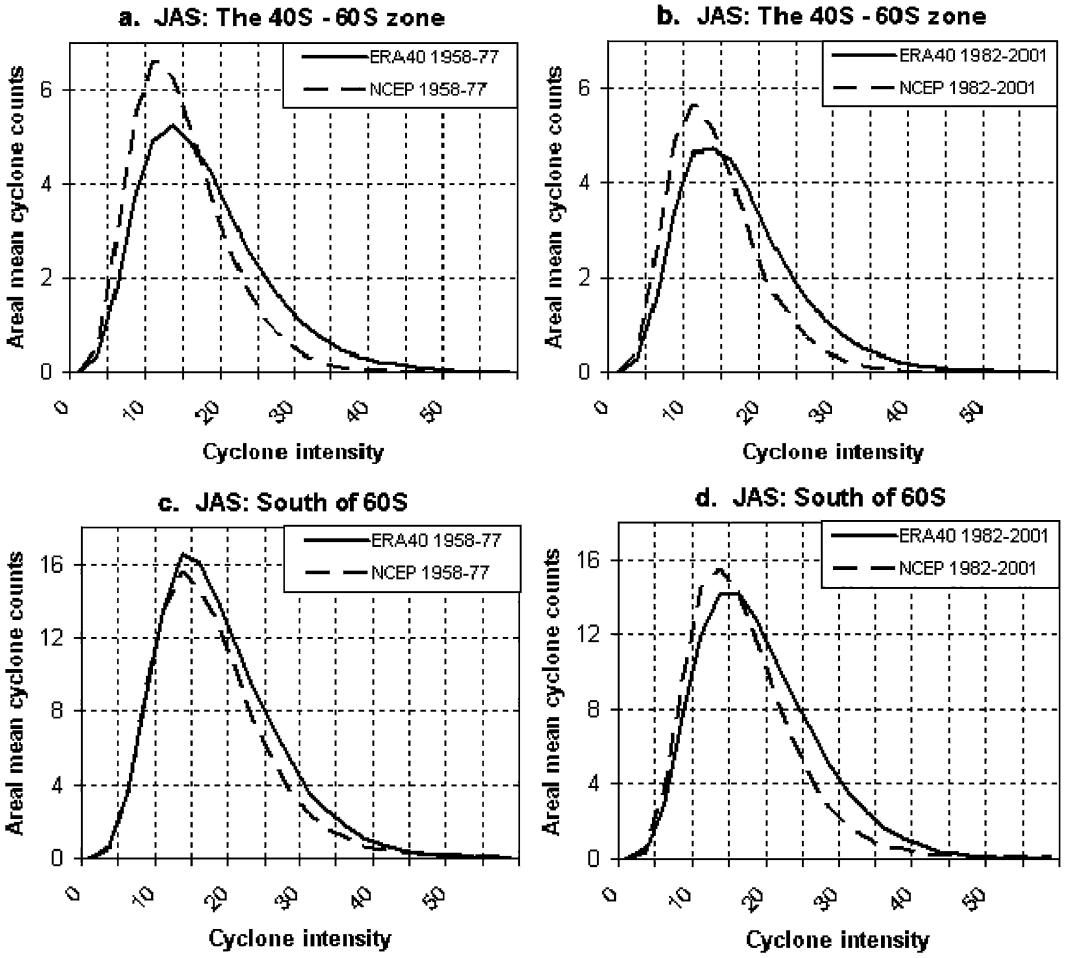

FIG. 7. Distributions of areal mean seasonal (JAS) cyclone counts vs. cyclone intensity for (a), (b) the 40°–60°S zone and (c), (d) the austral circumpolar region for the (left) first and (right) last 20-yr periods of the reanalyses. The unit of cyclone intensity is 10^{-5} hPa km^{-2}. ERA-40 shown by solid curve and NCEP by dashed curve.

desic distance measure (see Hodges et al. 2003 for the details). Since there will occasionally be more than one track in the NNR ensemble that satisfies the temporal matching threshold, the one with the least mean separation was taken to be the matching track.

As shown in the upper-left panel of Fig. 9, the median of the mean separation distances between the matching tracks is between 0.6° and 0.8° in the NH and between 1.4° and 1.6° in the SH. About 93% of the matching tracks in winter have a mean separation distance <2.0° in the NH and about 54% in the SH. For both NH and SH, the distributions of the mean separation distances are quite different from those in Hodges et al. (2003). This is probably due to the use of unfiltered MSLP of lower spatial resolution (on a 2.5°-by-2.5° latitude–longitude grid; versus filtered 850-hPa vorticity on a 1°-by-1° latitude–longitude grid used in Hodges et al. 2003). In this case, it makes little sense to define the best match using the distance threshold of 0.5° as in Hodges et al. (2003). Thus, we relaxed the spatial constraint, using a larger threshold of 2.0°. That is, if the mean separation distance between the pair of matching cyclone tracks is less than 2.0°, this is considered the best match.

The frequency distributions of the point-to-point intensity differences between the best-match tracks in the winter season of each hemisphere are shown in the upper-right panel of Fig. 9. Note that a negative intensity difference indicates that the ERA-40 cyclone track is stronger than the matching NNR cyclone track. Consistent with what is reported by Hodges et al. (2003), the distribution is much wider in the SH than in the NH, indicating greater uncertainty in the systems' intensities between the two reanalyses in the SH. There are about

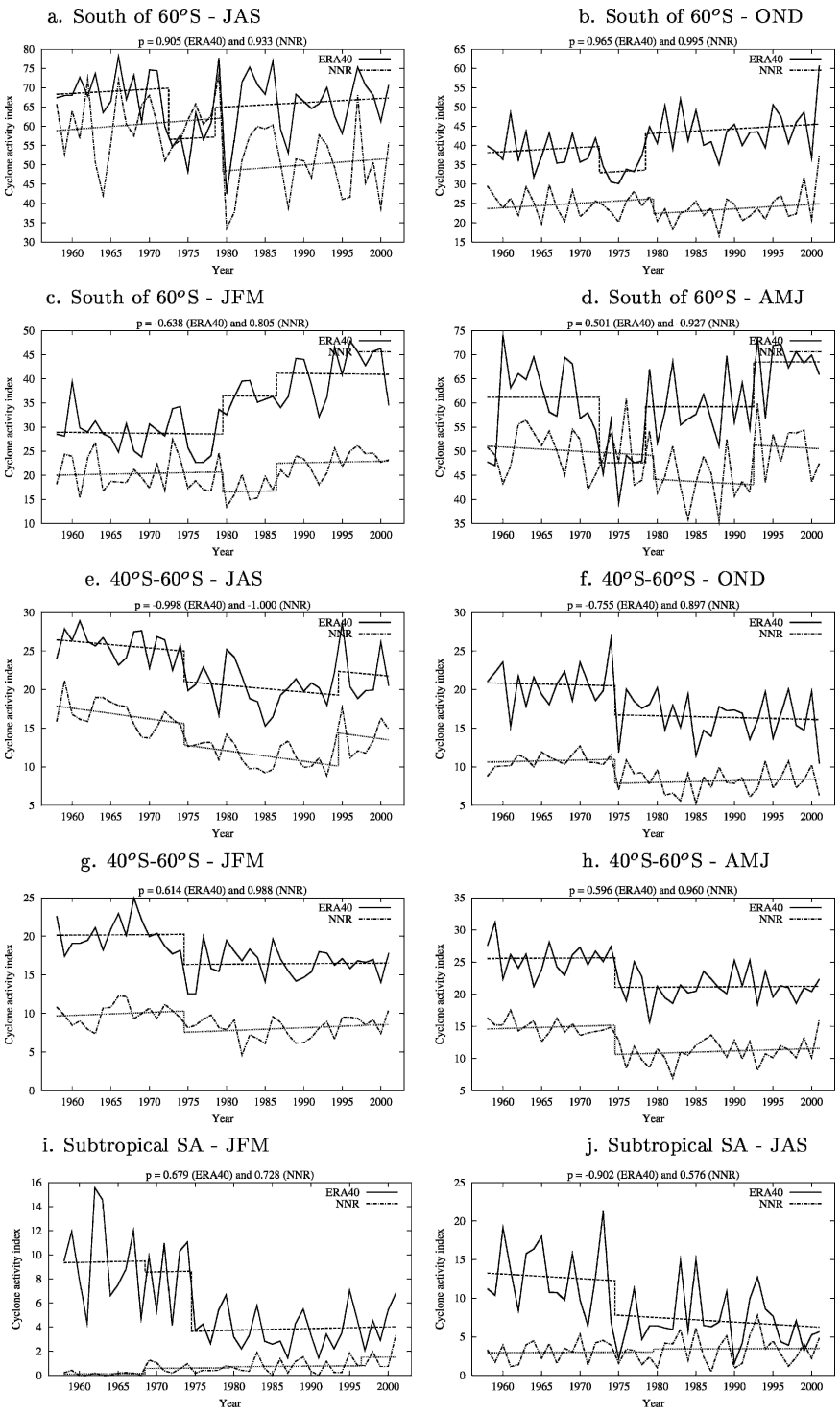

FIG. 8. Same as in Fig. 5, but for (a)–(d) the austral circumpolar region, (e)–(h) the 40°–60°S zone, and (i)–(j) the subtropical South Atlantic.

80% of the intensity differences that are between −1 and 1 unit in the NH, and only about 45% in the SH. In particular, there are more negative differences in the SH than in the NH (cf. the upper-right panel of Fig. 9), indicating that ERA-40 shows notably stronger cyclone activity in the SH than does NNR, which is consistent with what was revealed in section 3.

For the best-match tracks (i.e., those that satisfy both

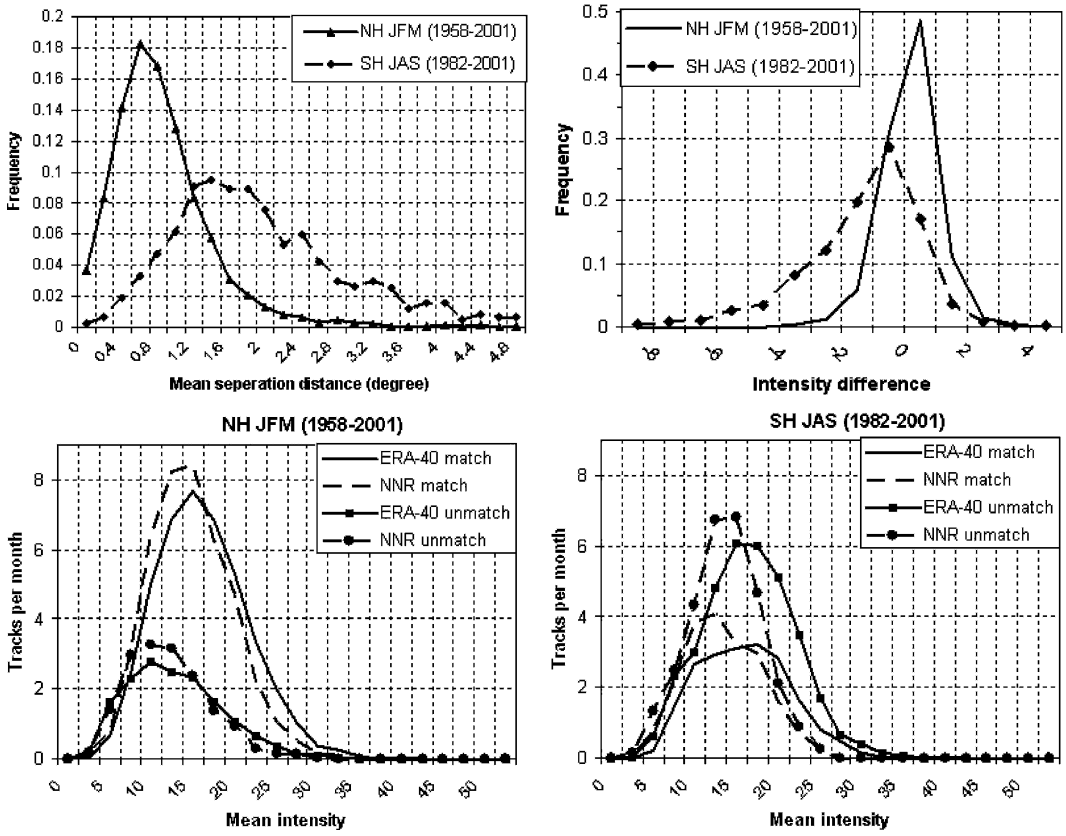

FIG. 9. (top) Cyclonic MSLP frequency distributions of (left) mean separation distances between the matching cyclone tracks and (right) of point-by-point intensity differences between the best-match cyclone tracks (i.e., with the mean separation distance $\leq 2°$). (bottom) Distributions of winter cyclone track mean intensity for the indicated groups of cyclone tracks: (left) Northern Hemisphere JFM and (right) Southern Hemisphere JAS. The intensity unit is 10^{-5} hPa km^{-2}.

the temporal and spatial constraints), the mean intensities for each track are computed and used to construct distributions of monthly track numbers over the mean intensity. This is also done for those tracks that do not match (i.e., all but the best-match tracks). These distributions are shown in the lower panels of Fig. 9 for the winter season of each hemisphere. In general, the best-match tracks are typically those with the larger mean intensities and those that do not match tend to be those with the weaker mean intensities. This is consistent with what is reported by Hodges et al. (2003). However, the distribution differences between those that match and those that do not match are slightly larger than those shown in Hodges et al. (2003), especially in the SH. Note that, in the presatellite era, there are few best-match tracks in the SH (the total number of best matches in the SH is generally less than three per month before 1973, and less than six per month during 1973–78). Thus, the lower-right panel of Fig. 9 shows the distribution for tracks identified in the period 1982–2001 (not the 44-yr period). Even in these recent decades, there are notably fewer tracks that match than those that do not match, which is different from what is shown in Hodges et al. (2003). This is likely related to the differences in data type and resolution and the spatial constraint used, in addition to the differences in the definition of seasons. Note that the use of the cyclone detection threshold of 1.0 hPa may also contribute to the above differences, and to the generally smaller numbers of tracks per month.

5. Historical climate changes

In this section, we compare the cyclone activity climatology for two 20-yr periods (1958–77 and 1982–2001) to characterize historical climate changes in the extratropical cyclone activity. This characterization is based mainly on ERA-40 and focuses on the cyclone activity index, cyclone occurrence frequency and its distribution over its intensity, and areal mean life span of cyclone tracks. Note that the reason for choosing the ERA-40 as the basis for showing historical changes is

that changes as derived from the NNR data have been shown in detail in many previous studies (e.g., Zhang et al. 2004; Fyfe 2003; Chang and Fu 2002; Gulev et al. 2001; Graham and Diaz 2001; Simmonds and Keay 2000). The presentation of changes derived from the ERA-40 data makes it possible for readers to compare them with changes derived from the NNR data in more detail than the comparison provided in this study. Nevertheless, ERA-40 cyclone activity is also briefly compared with NNR cyclone activity in terms of trend. For both reanalyses, the time series of seasonal counts and areal mean activity index of strong cyclones are also analyzed to assess trends and possible temporal discontinuities therein.

a. Changes over the boreal extratropics

Over the boreal extratropics, generally, larger changes were found to be associated with strong-cyclone activity. The most organized pattern of change is seen in winter (JFM), which is characterized by increases over the high-latitude North Atlantic, with decreases over the midlatitude North Atlantic and over eastern North America (Fig. 10a). In this season, increases are also seen over most areas of the North Pacific, with decreases along the East Asia coast (Fig. 10a). In the other seasons, changes do not have an organized pattern and are mostly not statistically significant at the 5% level (cf. Fig. 10b); the most extensive changes include spring (AMJ) increases over the northeastern Pacific and autumn (OND) increases over the Barent Sea, the Frame Strait (just east of Greenland), and the region south of Iceland (not shown).

As shown in Fig. 11a, the winter changes over the North Atlantic are associated with the storm track extending southeastward toward the North Sea while shrinking slightly northward over the northeastern Atlantic (10°–50°W; as can be seen by comparing the yellow edges with solid contour lines, or the red edges with the dashed contour lines in Fig. 11a). From period 1958–77 to period 1982–2001, the winter storm track, as defined by the activity index weighted mean latitudes of strong cyclones identified from ERA-40 within each 10° longitude band, shifted about 181 km northward over the North Atlantic (averaged over 10°E–60°W) and about 259 km northward over central Canada (averaged over 120°–70°W; see the blue and green curves in Fig. 11a).

Changes associated with weak-cyclone activity over the boreal extratropics are much smaller than, and often of opposite sign to, those associated with strong-cyclone activity. For example, as shown in Fig. 12a, the increase in winter cyclone activity over the high-latitude North Atlantic is mainly associated with strong cyclones (of intensity ≥15 units), with little change (or small decreases) associated with weak cyclones. Over the high-latitude North Atlantic in OND or over the midlatitude North Pacific in AMJ, changes associated

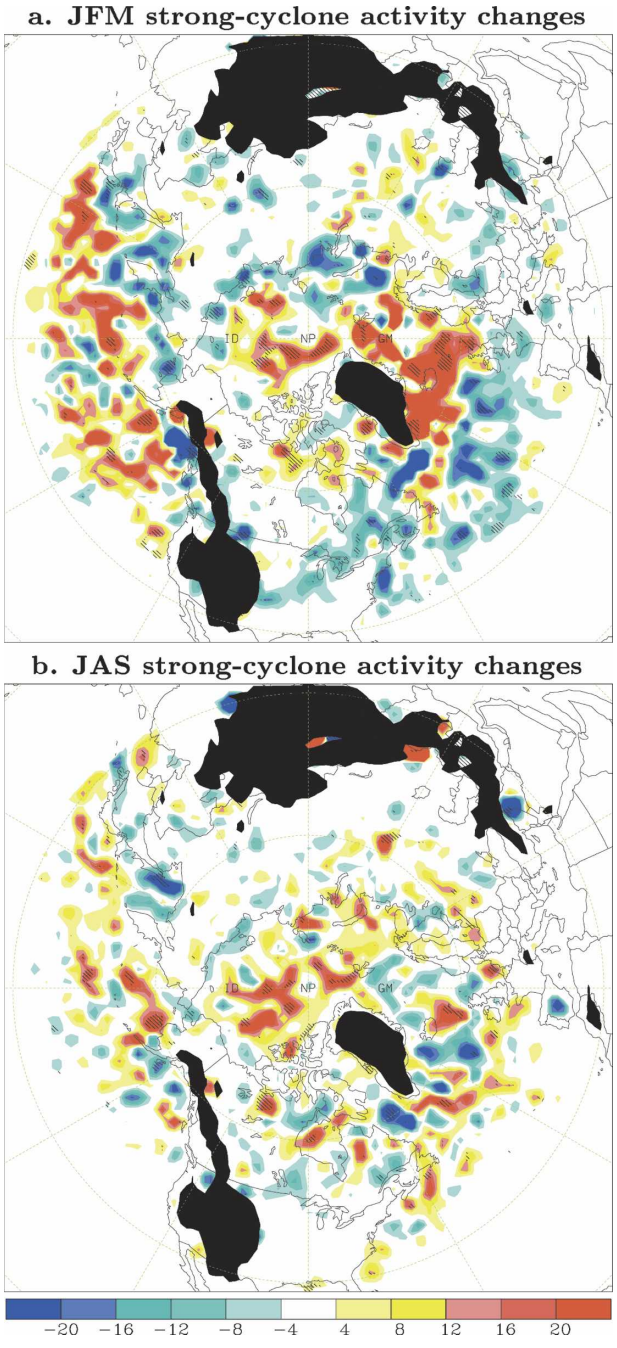

FIG. 10. Differences (10^{-5} hPa km^{-2}) of the strong-cyclone activity indices between two 20-yr periods 1958–77 and 1982–2001, as derived from ERA-40 data for the boreal extratropics: (a) JFM and (b) JAS. Red (blue) colors indicate increases (decreases) of strong-cyclone activity in period 1982–2001 relative to period 1958–77. Hatching indicates changes of at least 5% significance. Black-shaded areas are elevated areas (with elevation ≥1000 m).

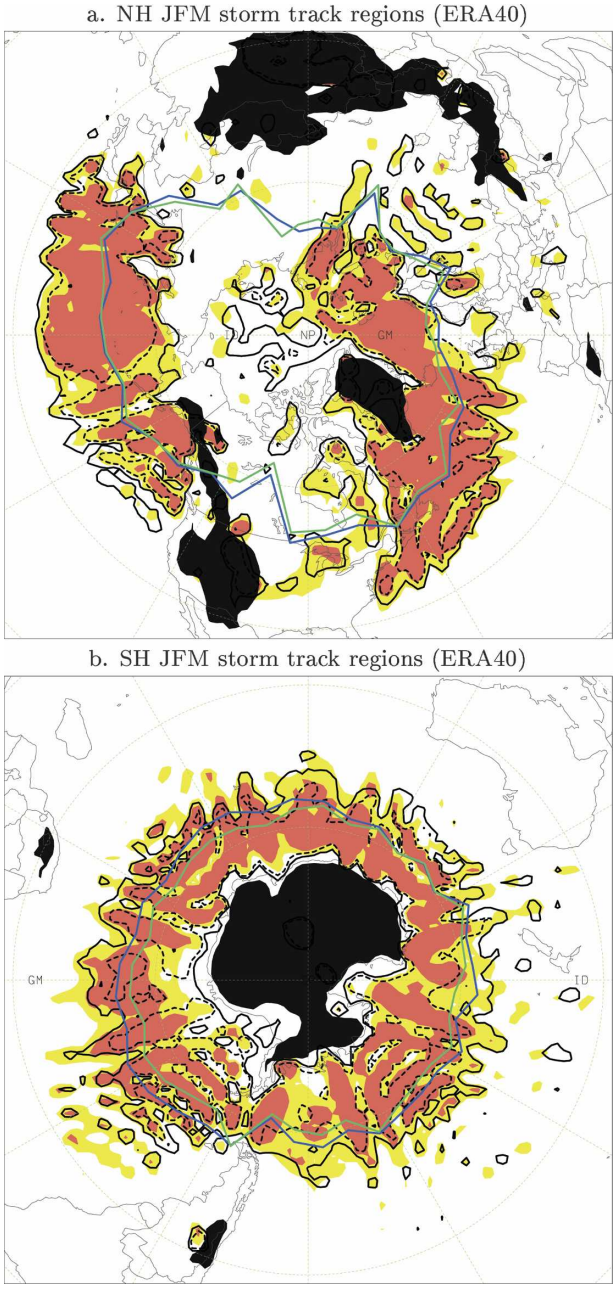

FIG. 11. Extratropical JFM storm track regions, as represented by contours of the 20-yr mean JFM strong-cyclone activity index for the period 1958–77 (shading contours) and the period 1982–2001 (line contours): (top) Northern Hemisphere (NH) and (bottom) Southern Hemisphere (SH). The yellow shading and the solid line contours represent the activity index of 20 units, and the red shading and the dashed line contours represent 40 units for the NH (or 15 and 30 units, respectively, for the SH; the unit is 10^{-5} hPa km^{-2}). The blue and green curves represent the mean positions of storm tracks, as defined by the activity index weighted mean latitudes of strong cyclones identified from ERA-40 (within each 10° longitude band) for periods 1958–77 (blue curve) and 1982–2001 (green curve), respectively.

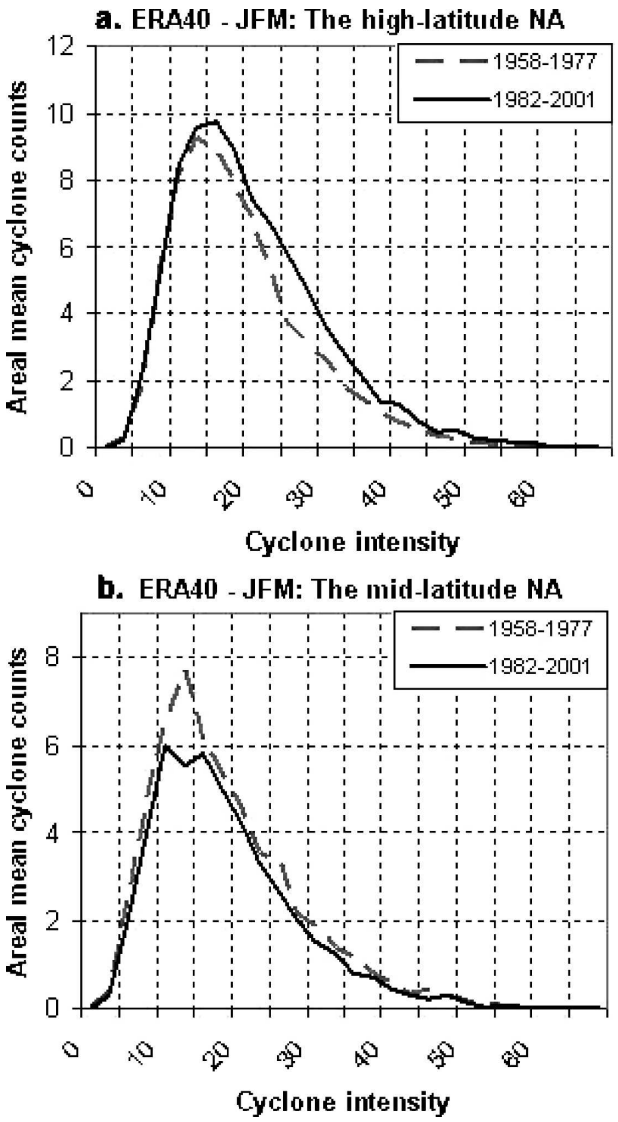

FIG. 12. Areal mean seasonal counts of cyclones as a function of their intensity (local Laplacian of pressure), as derived from 6-hourly MSLP data of the ERA-40 reanalysis for the two 20-yr periods 1958–77 (broken curve) and 1982–2001 (solid curve): (top) high-latitude and (b) midlatitude North Atlantic. The unit of cyclone intensity is 10^{-5} hPa km^{-2}.

with weak-cyclone activity are of the opposite sign to those associated with strong-cyclone activity (not shown). However, the decrease over the midlatitude North Atlantic is associated with cyclones of all intensity categories (Fig. 12b).

The pattern of change in winter strong-cyclone activity shown in Fig. 10a bears substantial similarity to the pattern of linear trends in the frequency of intense winter cyclones shown in Gulev et al. (2001, see their Fig. 5d), although they applied a different cyclone tracking algorithm on the NNR MSLP fields for 1958–99 (i.e.,

both the tracking algorithm and the data are different). Over the North Atlantic, the changes shown in Fig. 10a are also very similar to the pattern of trends reported by Geng and Sugi (2001, see their Figs. 2–3), who applied a different tracking algorithm and different analysis methods on the NNR MSLP fields for 1958–98. Based on the operational analyses of the National Meteorological Center (NMC), Lambert (1996) also reported that there is a noticeable increase in the number of intense winter cyclones in both the North Atlantic and the North Pacific sectors after 1970 (see Fig. 2 of Lambert 1996). In general, changes in the boreal extratropical cyclone activity as derived from the ERA-40 MSLP data are similar to those derived from the NNR MSLP data. This is also evident in the trends shown earlier in Fig. 5.

By analyzing cyclone-related 3-hourly sea level pressure changes observed at 83 Canadian stations for the 50-yr period of 1953–2002, Wang et al. (2006) also showed that winter cyclone activity has become more frequent, more durable, and stronger over the lower Canadian Arctic, but less frequent and weaker in southern Canada (their pattern of change is similar to that shown in Fig. 10a for Canada). Harnik and Chang (2003) compare storm-track variations as seen in radiosonde observations and NNR data and report that sonde data do show a positive trend over Canada, consistent with a Pacific storm-track intensification and northeastward shift. The consistency of the changes identified from ERA-40 data with those from radiosonde data and from the Canadian in situ data suggests that the changes are most likely real for the Canadian region, not just an artifact of the reanalysis procedure or of the increasing availability of data (including satellite data) in the recent decades. Perhaps, such a consistency can also be expected for other areas with reasonable in situ data coverage throughout the reanalysis period. For example, using the NNR 6-hourly MSLP (and winds) data for the winter months (December–March) from 1948/49 to 1997/98, Graham and Diaz (2001) found evidence of a southward dip and eastward extension of the North Pacific storm track (and increased frequency of deep lows accompanied with decreased minimum central pressure). In particular, they also found support for the changes described above from analyzing long-term quality-controlled in situ datasets, including the Comprehensive Ocean–Atmosphere Data Set (COADS; Woodruff et al. 1987), Midway Island (28°N, 177°W) radiosonde observations, and observations from two Ocean Station Vessels (or "weather ships") in the region. However, Chang (2005) and Harnik and Chang (2003) report that the increase in the Pacific storm track during the second half of the twentieth century may not be as large as suggested by the NNR data (e.g., in Graham and Diaz 2001). Harnik and Chang (2003) also report that the Atlantic storm track intensified during the 1960s to 1990s, although the intensification suggested by sonde data was weaker than that suggested by NNR. The larger trend in reanalysis data is due to the increase in frequency of observations over time and a decreasing trend in observational error statistics (Chang 2005).

By referring back to Fig. 5, we also see evidence supporting the veracity of the JFM changes over the boreal oceans. Namely, there is no apparent data inhomogeneity (sudden jumps/drops in the mean) in these time series, while the JFM strong-cyclone activity has significantly decreased over the midlatitude North Atlantic but increased over the high-latitude North Atlantic and the midlatitude North Pacific (Figs. 5a,b,d).

Changes in the number of cyclones are generally consistent with changes in the number of cyclone tracks. As shown in Table 2, over the midlatitudes of the North Atlantic, the number of weak-cyclone tracks has significantly decreased in JFM but increased in AMJ, with insignificant changes in the number of strong-cyclone tracks (see Table 2 for the definition). In the other areas, however, changes in the number of strong-cyclone tracks are generally more significant than those in the number of weak-cyclone tracks. A significant increase in the number of strong-cyclone tracks was identified for the midlatitude North Pacific in OND, with a marginally significant increase in AMJ and JAS. Over the entire boreal middle to high latitudes, there is also a marginally significant increase in the number of strong-cyclone tracks in both OND and JFM, with insignificant changes in the number of weak-cyclone tracks (Table 2). In JAS, the changes are generally small and insignificant and so are the AMJ changes over the high latitudes of the North Atlantic (Table 2).

However, changes in the areal mean life span of cyclone tracks are largest in JAS, with a significant increase over the North Atlantic and a marginally significant increase over the midlatitude North Pacific, as shown in Table 3. All North Atlantic summer (JAS) cyclone tracks, strong or weak, have a longer life span in the recent than in the early decades, and so do the midlatitude North Pacific winter (JFM) strong-cyclone tracks (Table 3). The midlatitude North Atlantic spring (AMJ) strong-cyclone tracks also seems to live longer in the recent than in the early decades, although the life span increase is not statistically significant (Table 3). Note that a notable increase in life span is usually associated with very small, insignificant changes in the number of cyclone tracks; while no significant change in the life span was identified for the regions of significant

TABLE 2. Changes in the counts of cyclone tracks with life span ≥24 h, as identified in the indicated regions from the ERA-40 reanalysis (1982–2001 minus 1958–77; the numbers in parentheses are the total counts for the two 20-yr periods). Changes of 5% and 20% significance are in bold and underlined, respectively (results of two-sided Student's *t* tests at the 2.5% and 10% levels in each tail). Note that a strong-cyclone track is defined as one having the local Laplacian of pressure $\geq 15 \times 10^{-5}$ hPa km^{-2} at least once in its lifetime within the selected region, and that a cyclone track could be counted twice if its life span traverses two consecutive seasons (it gets counted in both seasons; thus, the annual count may be smaller than the sum of the relevant four seasonal counts).

Cyclone detection threshold			High-latitude NA (55°–70°N, 45°W–15°E)	Midlatitude NA (45°–55°N, 75°–10°W)	Midlatitude NP (35°–50°N, 125°W–140°E)	Boreal middle to high latitudes (≥30°N)
1.0 hPa	OND	Strong	41 (261–220)	30 (233–203)	68 (317–249)	52 (396–344)
		Weak	−3 (605–608)	−18 (704–722)	−32 (936–968)	91 (7360–7269)
		All	38 (866–828)	12 (937–925)	36 (1253–1217)	143 (7756–7613)
	JFM	Strong	44 (304–260)	13 (287–274)	24 (335–311)	60 (523–463)
		Weak	14 (576–562)	**−100** (682–782)	35 (1128–1093)	−40 (7484–7524)
		All	58 (880–822)	**−87** (969–1056)	59 (1463–1404)	20 (8007–7987)
	AMJ	Strong	4 (86–82)	−12 (86–98)	21 (96–75)	−4 (281–285)
		Weak	7 (657–650)	**98** (869–771)	28 (991–963)	**211** (8724–8513)
		All	11 (743–732)	**86** (955–869)	**49** (1087–1038)	207 (9005–8798)
	JAS	Strong	0 (59–59)	9 (70–61)	11 (51–40)	−10 (227–237)
		Weak	−15 (669–684)	2 (734–732)	−23 (823–846)	105 (7977–7872)
		All	−15 (728–743)	11 (804–793)	−12 (874–886)	95 (8204–8109)
	ANN	Strong	93 (694–601)	37 (660–623)	**118** (773–655)	89 (1336–1247)
		Weak	5 (2485–2480	−20 (2957–2977)	2 (3833–3831)	327 (30949–30622)
		All	98 (3179–3081)	17 (3617–3600)	120 (4606–4486)	416 (32285–31869)
0.2 hPa	OND	Strong	33 (243–210)	28 (205–177)	**77** (277–200)	**53** (309–256)
		Weak	1 (756–755)	**−2** (885–887)	−30 (1223–1253)	**387** (10696–10309)
		All	34 (999–965)	26 (1090–1064)	47 (1500–1453)	**440** (11005–10565)
	JFM	Strong	57 (286–229)	25 (269–244)	23 (284–261)	11 (376–368)
		Weak	35 (765–730)	**−124** (858–982)	5 (1402–1397)	28 (10846–10818)
		All	92 (1051–959)	**−99** (1127–1226)	28 (1686–1658)	39 (11225–11186)
	AMJ	Strong	6 (69–63)	−8 (76–84)	8 (77–69)	8 (190–182)
		Weak	51 (919–868)	**66** (1077–1011)	55 (1042–1397)	271 (13222–12951)
		All	57 (988–931)	58 (1153–1095)	63 (1317–1254)	279 (13222–12951)
	JAS	Strong	−1 (51–52)	1 (48–47)	6 (40–34)	−3 (129–132)
		Weak	−22 (937–959)	17 (958–941)	−1 (1133–1134)	165 (12873–12708)
		All	−23 (988–1011)	18 (1006–988)	5 (1173–1168)	162 (13002–12840)
	ANN	Strong	**97** (634–537)	48 (584–536)	**105** (652–547)	64 (926–862)
		Weak	63 (3344–3281)	−4.8 (3731–3779)	3.6 (4942–4906)	**780** (46700–45920)
		All	**160** (3978–3818)	0 (4315–4315)	141 (5594–5453)	**844** (47626–46782)

changes in the number of cyclone tracks (cf. Tables 2–3). Also, cyclones over the elevated areas were excluded from the calculation of the statistics shown in Tables 2–3.

Use of higher spatial/temporal resolution data would lead to more accurate estimates of the count and mean life span of cyclone tracks. For example, in the second period (1982–2001), satellite and much more aircraft observations were assimilated, and there are many more buoy observations in the SH; hence it is conceivable that cyclones are observed earlier in their life cycle, and there is more continuity in the track of cyclones, since there are observations more or less continuously to update the positions of cyclones. During the early period, however, there are much fewer observations, and hence cyclones in the reanalyses could conceivably be much more "jumpy," since their positions and intensity are only updated sporadically by observations; thus their "analyzed" track could be much more erratic than the real track, which could lead to a low bias in the analyzed life span. The choice of the cyclone detection threshold value could also have an impact in this regard. To assess the sensitivity of the count and life span estimates to the choice of cyclone detection threshold, we also repeated the analysis using a cyclone detection threshold of 0.2 hPa (instead of 1.0 hPa). As shown in Tables 2–3, in most cases, we obtained qualitatively consistent results, although the individual numbers can differ. In other words, the qualitative conclusions drawn from Tables 2–3 above are generally not significantly affected by the change in the cyclone detection threshold. However, there is some uncertainty in the results shown in Table 3. For example, for the areal mean life span of AMJ strong cyclones over the high-

TABLE 3. Same as in Table 2, but for changes in the areal mean life span (h) of cyclone tracks identified in the indicated regions from the ERA-40 reanalysis (1982–2001 minus 1958–77). Changes of 5% (20%) significance are in bold (underlined).

Cyclone detection threshold			High-latitude NA (55°–70°N, 45°W–15°E)	Midlatitude NA (45°–55°N, 75°–10°W)	Midlatitude NP (35°–50°N, 125°W–140°E)	Boreal middle to high latitudes (≥30°N)
	OND	Strong	1.8 (88.7–86.9)	0.6 (88.6–88.0)	−0.6 (87.5–88.1)	1.8 (47.9–46.1)
		All	−0.3 (93.3–93.6)	−2.8 (92.4–95.2)	2.9 (90.2–87.3)	0.2 (66.9–66.7)
	JFM	Strong	−3.6 (81.4–85.0)	3.7 (89.2–85.5)	**9.6** (91.7–82.1)	1.6(43.2–41.6)
		All	0.6 (88.1–87.5)	−0.9 (87.6–88.5)	2.7 (86.0–83.3)	0.4 (62.7–62.3)
1.0 hPa	AMJ	Strong	11.5 (99.0–87.5)	6.2 (105.1–98.9)	−5.3 (101.4–106.7)	−0.4 (62.7–63.1)
		All	0.8 (97.5–96.7)	−1.3 (98.0–99.3)	−0.8 (96.3–97.1)	0.4 (67.7–67.3)
	JAS	Strong	8.1 (99.9–91.8)	21.2 (141.2–120.0)	0.8 (142.4–141.6)	−2.7 (68.3–71.0)
		All	**9.7**(109.5–99.8)	**8.1**(106.4–98.3)	7.4 (104.3–96.9)	2.0 (73.9–71.9)
	ANN	Strong	0.1 (86.4–86.3)	4.8 (95.4–90.6)	3.8 (92.7–88.9)	−1.4 (49.1–50.5)
		All	2.4 (95.8–93.4)	0.7 (95.0–94.3)	**2.7** (92.0–89.3)	0.7 (66.9–66.2)
	OND	Strong	3.9 (97.2–93.3)	−0.2 (99.4–99.6)	2.8 (99.2–96.4)	−5.1 (48.6–53.7)
		All	0.7 (96.4–95.7)	−4.4 (96.3–100.7)	2.3 (93.0–90.7)	−0.6 (66.2–66.8)
	JFM	Strong	−1.3 (84.8–86.1)	3.7 (97.9–94.2)	7.5 (101.6–94.1)	1.1 (42.4–41.3)
		All	0.0 (89.0–89.0)	−0.4 (90.4–90.8)	2.6 (88.0–85.4)	0.6 (62.3–61.7)
0.2 hPa	AMJ	Strong	−19.4 (95.5–114.9)	7.8 (119.9–112.1)	1.4 (122.7–121.3)	−0.8 (100.5–101.3)
		All	−2.8 (97.0–99.8)	0.6 (103.1–102.5)	−2.3 (101.7–104.0)	0.6 (70.7–70.1)
	JAS	Strong	20.2 (120.8–100.6)	19.8 (159.7–139.9)	28.5 (189.2–160.7)	−23.0 (98.6–121.6)
		All	**10.1** (110.1–100.0)	**9.7** (114.9–105.2)	5.4 (109.5–104.1)	**1.9** (76.5–74.6)
	ANN	Strong	−1.1 (91.8–92.9)	2.2 (104.6–102.4)	5.9 (105.7–99.8)	−5.5 (57.5–63.0)
		All	2.0 (97.4–95.4)	1.4 (100.1–98.7)	1.9 (95.8–93.9)	0.7 (68.2–67.5)

latitude North Atlantic, a large but insignificant increase was estimated using the 1.0-hPa detection threshold, while a marginally significant decrease was estimated using the 0.2-hPa detection threshold.

b. Changes over the austral extratropics

As shown in Fig. 13, strong-cyclone activity over a narrow zone around the Antarctic coast has increased significantly in all four seasons, with significant decreases over most areas to the north of this zone. Among the four seasons, the increase is most extensive in JFM, and least extensive in JAS, while more extensive decreases are seen over the South Atlantic in OND and JFM, but over the South Pacific in AMJ and JAS (Fig. 13). The changes over the austral extratropics are associated with a poleward shift of the storm tracks, which is seen in all seasons but is most notable in JFM (cf. Fig. 11b). However, the estimates of change shown in Fig. 13 are heavily biased by data inhomogeneities (see discussions after the next paragraph).

Just like in the boreal extratropics, changes associated with weak cyclones in the austral extratropics are also much smaller. However, the austral weak cyclones have generally experienced slightly more extensive changes than the boreal counterpart. In the warm seasons (JFM and OND), the increase in the number of strong cyclones over the austral high latitudes was accompanied by a decrease in the number of weak cyclones, while in JAS larger changes are found to be associated with cyclones of weak and moderately strong intensity (cf. Fig. 14). Note that we also see a decrease in the number of moderately strong cyclones (intensity of 15–30 units) in Fig. 14b, which indicates that the increases in JAS strong-cyclone activity near the Antarctic were overwhelmed by the decreases in the rest of the austral circumpolar region (see Fig. 13b). The decrease over the austral midlatitudes is larger for the strong cyclones but can be seen for cyclones of all intensity categories (not shown; but similar to Fig. 14b, with slightly larger changes in both tails).

However, as shown earlier in Fig. 8, there exist abrupt changes in the time series of the areal mean seasonal strong-cyclone activity index, which appear to be related to the increasing availability of data during the reanalysis period. These abrupt changes could affect the estimates of trend. We have tried to diminish such effects by means of a two- or multiphase regression analysis (see the appendix) that was proposed by Wang and Feng (2004) and Wang (2003), and used recently in Wang (2006) and Hanesiak and Wang (2005). Our estimates of abrupt changes and trends are shown earlier in Fig. 8. In particular, the JFM increase in the austral circumpolar region is not statistically significant if artificial upward jumps are taken into account in the trend analysis (see Fig. 8c). Consistent with this is that Bengtsson et al. (2004) also report an upward jump around 1978/79 in the global total kinetic energy derived from ERA-40, which is bigger for the southern

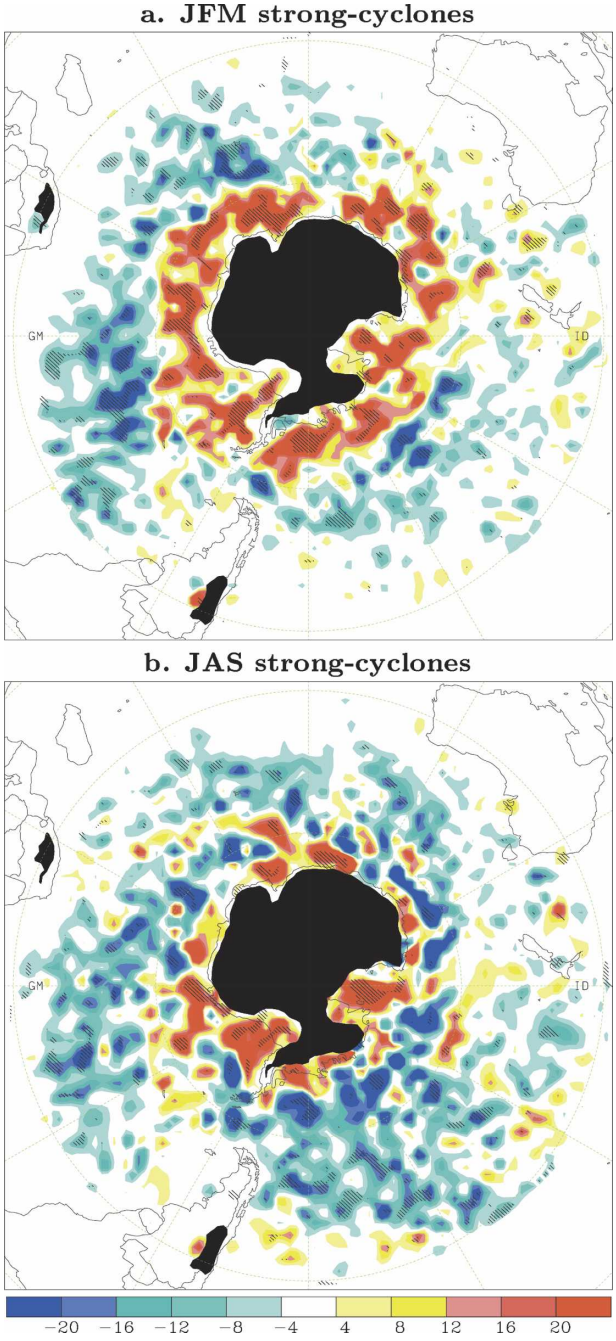

FIG. 13. Same as in Fig. 10, but for the austral extratropics.

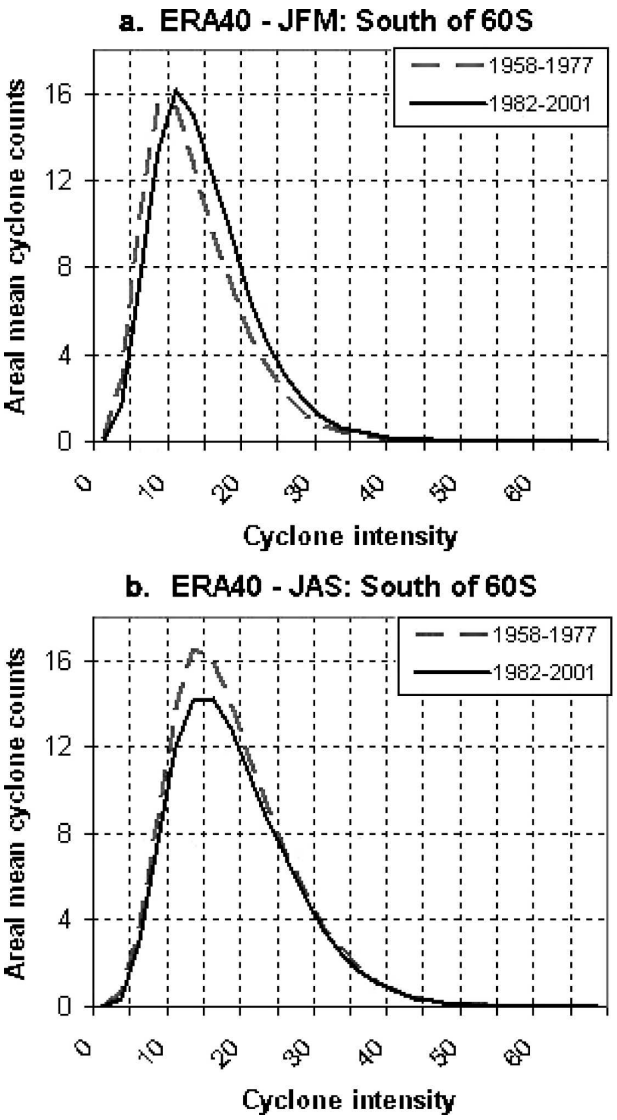

FIG. 14. Same as in Fig. 12, but for the austral circumpolar region.

extratropics and largest in DJF in both hemispheres. Their analysis also suggests that the jump is an artifact caused by changes in the global observing system. Note that Bengtsson et al. (2004) discuss the austral extratropics as a whole, while we separate the austral circumpolar region from the austral midlatitudes (40°–60°S) in this study. The downward jumps we identified for the 40°–60°S zone were not evident in the results of Bengtsson et al. (2004). Also, our data "homogenization" technique assumes a common linear trend throughout the 44-yr period, which might be unrealistic here, because the rate of change simulated by the model only (with little constraint by observations) for the presatellite era could be different from the rate of change obtained when the model is constrained by observations for the postsatellite era. However, this is just one way to interpret the data, and there is a need to analyze alternative data that can act as an independent check for whether these estimates of the jumps and trends are realistic or not. It is probably not wise to take these trends too seriously, until such time when these jumps can be justified (in terms of both sign and magnitude) by other independent data sources.

Nevertheless, the results of the multiphase regression analysis show that, in general, ERA-40 shows trends of a lower significance level than does NNR over the austral extratropics (Fig. 8). More specifically, over the austral circumpolar region, ERA-40 and NNR show similar trends in JAS and OND, but small trends of opposite signs in the other seasons (Figs. 8a–d). For both reanalyses, the increase in the areal mean strong-cyclone activity index is statistically significant (i.e., with the p value > 0.95) in OND and is of a marginal significance (i.e., $0.80 < p \leq 0.95$) in JAS (Figs. 8a–b). Over the 40°–60°S zone, consistently, both reanalyses show a statistically significant decreasing trend in JAS (Fig. 8e). However, ERA-40 shows no significant change in JFM and AMJ, while NNR shows a significant increasing trend in these seasons (Figs. 8g–h).

In terms of trend, the largest differences between ERA-40 and NNR are seen over the subtropical (30°–45°S) South Atlantic and the subtropical South Pacific (see Fig. 3b for their boundaries). ERA-40 shows a much larger decreasing trend than does NNR over the subtropical South Atlantic in AMJ, and over the subtropical South Pacific in OND and AMJ (not shown); while both reanalyses show no significant changes in these regions in JFM (cf. Fig. 8j). In particular, ERA-40 and NNR show trends of the opposite signs over the subtropical South Atlantic in JAS and OND (cf. Fig. 8j), and over the subtropical South Pacific in JAS (not shown).

Simmonds and Keay (2000) did a comprehensive study on variability of extratropical Southern Hemisphere cyclone behavior by applying a state-of-the-art cyclone finding and tracking scheme (similar to the one used in this study) to the 6-hourly NNR data for 1958–97. They showed that the annual and seasonal mean cyclone densities (number of cyclones per unit area) have decreased at most locations between 40° and 70°S, and increased to the north and over the Antarctic, and that the trends in seasonal cyclone counts are steeper in the cold than in the warm seasons. However, their analysis was based on the uncorrected NNR data; hence, their estimates of trends are contaminated by the presence of significant data inhomogeneity, although their results have a little qualitative consistency with the results shown in this study (e.g., both studies show a negative trend in the austral midlatitudes).

6. Concluding remarks

By applying a cyclone finding/tracking algorithm to two gridded global 6-hourly MSLP datasets, we have compared the ERA-40 cyclone activity climatology and climatic changes with those of NNR.

The results show that, in terms of cyclone activity climatology and trends therein, ERA-40 and NNR are in reasonably good agreement with each other over northern Europe and eastern North America, while ERA-40 shows systematically stronger cyclone activity over the boreal extratropical oceans than does NNR. Some significant differences were also identified over Siberia and over the north shore region of the Mediterranean in all seasons. In particular, ERA-40 shows significantly weaker cyclone activity over the leeside of the Rocky Mountains in all seasons, which may be attributable to the subgrid-scale orographic parameterization used in ERA-40. Differences between ERA-40 and NNR are much more extensively significant over the austral than over the boreal extratropics. In particular, ERA-40 shows significantly greater strong-cyclone activity and less weak-cyclone activity over all oceanic areas south of 40°S in all seasons, while it shows significantly stronger cyclone activity over most areas of the austral subtropics in the warm seasons. Over the austral circumpolar region, larger differences between the two reanalyses are seen in the last than in the first two decades of the reanalysis period. However, over the region north of 60°S, especially over the subtropical South Atlantic, much larger differences, which are largely due to data inhomogeneities, are seen in the first two decades.

Over both the austral and the boreal extratropics, ERA-40 shows systematically greater strong-cyclone activity than does NNR. This may be attributable to the high model resolution, updated data assimilation system, and more/improved observation data assimilated in ERA-40. Note that differences in model resolution might affect small-scale dynamics and cyclogenesis. In particular, higher spatial resolution models can better represent the extremes. Different model resolution also means different representation of the surface topography and hence different surface elevations (perhaps also algorithms) used to do the pressure reduction to the mean sea level. These kinds of systematic difference between models might lead to biases in the MSLP field that might affect cyclone climatologies.

In terms of historical trend, the most notable changes in cyclone activity were found to be associated with strong-cyclone activity. Over the boreal extratropics, consistently, both ERA-40 and NNR show a significant increasing trend in winter (JFM) strong-cyclone activity over the high-latitude North Atlantic and over the midlatitude North Pacific, with a significant decreasing trend over the midlatitude North Atlantic and a small increasing trend over northern Europe. The winter changes over the North Atlantic are associated with the

mean position of the storm track shifting about 181 km northward. Importantly, there is no evidence of abrupt changes in the time series of areal mean seasonal strong-cyclone activity index over the boreal extratropics, although it has been suggested that the upward trend in the boreal extratropical cyclone activity derived from the NNR data could be biased high (Chang 2005; Harnik and Chang 2003). However, there exist abrupt changes over the austral extratropics, which appear to be attributable to the increasing amount of observations assimilated in the reanalyses. After diminishing the effects of these abrupt changes, we identified from both reanalyses an increasing trend in strong-cyclone activity over the austral circumpolar oceanic region in OND and JAS, with a decreasing trend in strong-cyclone activity over the 40°–60°S zone in JAS.

For the boreal extratropics, the historical changes identified in this study are basically consistent with the findings of previous studies using different analysis methods and/or different datasets (in situ data or simulations of different climate models).

Acknowledgments. The authors are very grateful to Mark Serreze (University of Colorado, Boulder) for providing us with his cyclone identification/tracking program (FORTRAN codes) and useful advice regarding the use of the program. The authors are greatly indebted to Yang Feng for his excellent computing support and to Bin Yu and Walter Skinner for their useful internal review of an earlier version of this manuscript. The authors wish to thank the two anonymous reviewers for their constructive review comments.

APPENDIX

Data Homogeneity Test and Multiphase Regression Analysis

The homogeneity test for time series (say x_t) is the same as in Wang (2006), which is based on the following two-phase regression technique proposed by Wang (2003):

$$x_t = \begin{cases} \mu_1 + \beta t + \varepsilon_t, & N_1 \le t \le t_c \\ \mu_2 + \beta t + \varepsilon_t, & t_c < t \le N_2 \end{cases}, \qquad \text{(A1)}$$

where t_c denotes a possible point of artificial mean shift of size $\delta_c = (\mu_2 - \mu_1) \neq 0$, which divides the time series x_t for $t \in \{N_1, N_1 + 1, \ldots, N_2\}$ into two segments: $t \in \{N_1, N_1 + 1, \ldots, t_c\}$ and $t \in \{t_c + 1, t_c + 2, \ldots, N_2\}$ $(1 \le N_1 < N_2 \le N)$. For each and every trial value of $t_c \in \{N_1 + N_{\min}, N_1 + N_{\min} + 1, \ldots, N_2 - N_{\min}\}$ (where $N_{\min}$ is a selected minimum length of segment), the sum of squared errors (SSE) of model (A1) was compared with that of the following null model:

$$x_t = \mu + \beta t + \varepsilon_t, \quad 1 \le t \le N \qquad \text{(A2)}$$

(i.e., $\mu_1 = \mu_2 = \mu$; there is no mean shift). The time t_c that is associated with the maximum reduction in the SSE (among all the trial values of t_c) and statistically significant improvement in the fit of model (A1) [over model (A2)] is chosen as a possible changepoint (point of mean shift). As described in Wang (2006) and in Wang and Feng (2004), this procedure was repeated until all segments are either deemed to be homogeneous at the selected significance level or too short to be divided further (i.e., each segment has fewer than $2 \times N_{\min}$ data points, i.e., fewer than 6 data points in this study). During the process of detecting changepoints, visual inspection of the time series in question was carried out to help determine whether or not to include a changepoint in the time series; and metadata (in this case, it is the information that is provided in Tables 1–2 and Fig. 1 of Uppala et al. 2005) were used to check the veracity of the mean shifts detected. However, there exist "undocumented changepoints" (i.e., changepoints that were identified to be significant statistically and visually, but no metadata were available to verify them or no reason was found to explain them), which need to be and were accounted for. Of course, the appropriate (much higher) critical values, as correctly specified in Wang (2003), were used to identify undocumented changepoints (see also Lund and Reeves 2002).

Apparently, this data homogenization procedure includes some subjective analysis. However, such subjectivity is necessary because the so-called type I and type II errors (i.e., mistakenly reject and accept the null hypothesis of no mean shift) are inherent in any statistical test, which in this case means that there is always a small possibility for the statistical test to identify a changepoint that does not exist or fail to identify a real changepoint. The subjective checking or the time series visualization aims to reduce the inherent errors of statistical tests.

Then, if the time series in question was found to have no mean shift, model (A2) was used to estimate the trend β. If $K > 0$ points of artificial mean shifts were identified in the time series, a $(K + 1)$ phase regression model was fitted to the time series to estimate the trend β, as well as the size of the kth mean shift $\delta_k = (\mu_{k+1} - \mu_k)$ for $k = 1, 2, \ldots, K$. A Student's t test was then completed to determine whether the trend β was statistically different from zero, and to assess the statistical significance level of the estimated trend (von Storch and Zwiers 1999).

Readers are referred to Wang (2006), Wang and Feng (2004), and Hanesiak and Wang (2005) for more details about the time series homogenization technique/procedure and trend analysis.

REFERENCES

Anderson, D., K. I. Hodges, and B. J. Hoskins, 2003: Sensitivity of feature-based analysis methods of storm tracks to the form of background field removal. *Mon. Wea. Rev.,* **131,** 565–573.

Armstrong, R. L., and M. J. Brodzik, 1995: An earth-gridded SSM/I data set for cryospheric studies and global change monitoring. *Adv. Space Res.,* **16** (10), 155–163.

Bengtsson, L., S. Hagemann, and K. I. Hodges, 2004: Can climate trends be calculated from reanalysis data? *J. Geophys. Res.,* **109,** D11111, doi:10.1029/2004JD004536.

Blackmon, M. L., 1976: A climatological spectral study of the 500-mb geopotential height of the Northern Hemisphere. *J. Atmos. Sci.,* **33,** 1607–1623.

Cai, M., and M. Mak, 1990: Symbiotic relation between planetary and synoptic-scale waves. *J. Atmos. Sci.,* **47,** 2953–2968.

Chang, E. K. M., 2005: Effects of secular changes in frequency of observations and observational errors on monthly mean MSLP summary statistics derived from ICOADS. *J. Climate,* **18,** 3623–3633.

——, and Y. Fu, 2002: Interdecadal variations in Northern Hemisphere winter storm track intensity. *J. Climate,* **15,** 642–658.

——, and ——, 2003: Using mean flow change as a proxy to infer interdecadal storm track variability. *J. Climate,* **16,** 2178–2196.

——, S. Lee, and K. Swanson, 2002: Storm track dynamics. *J. Climate,* **15,** 2163–2183.

Fyfe, J. C., 2003: Extratropical Southern Hemisphere cyclones: Harbingers of climate change? *J. Climate,* **16,** 2802–2805.

Geng, Q., and M. Sugi, 2001: Variability of the North Atlantic cyclone activity in winter analyzed from NCEP–NCAR reanalysis data. *J. Climate,* **14,** 3863–3873.

Gibson, R., P. Kallberg, S. Uppala, A. Nomura, A. Hernandez, and E. Serrano, 1997: ERA description. ECMWF Re-Analysis Final Rep. Series 1, ECMWF, 71 pp.

Graham, N. E., and H. F. Diaz, 2001: Evidence for intensification of North Pacific winter cyclones since 1948. *Bull. Amer. Meteor. Soc.,* **82,** 1869–1893.

Gulev, S. K., O. Zolina, and S. Grigoriev, 2001: Extratropical cyclone variability in the Northern Hemisphere winter from the NCEP/NCAR reanalysis data. *Climate Dyn.,* **17,** 795–809.

Hanesiak, J. M., and X. L. Wang, 2005: Adverse-weather trends in the Canadian Arctic. *J. Climate,* **18,** 3140–3156.

Harnik, N., and E. K. M. Chang, 2003: Storm track variations as seen in radiosonde observations and reanalysis data. *J. Climate,* **16,** 480–495.

Hayden, B., 1981: Cyclone occurrence mapping: Equal area or raw frequencies? *Mon. Wea. Rev.,* **109,** 168–172.

Hodges, K. I., B. J. Hoskins, J. Boyle, and C. Thorncroft, 2003: A comparison of recent reanalysis datasets using objective feature tracking: Storm tracks and tropical easterly waves. *Mon. Wea. Rev.,* **131,** 2012–2037.

Hoskins, B. J., and K. I. Hodges, 2002: New perspectives on the Northern Hemisphere winter storm tracks. *J. Atmos. Sci.,* **59,** 1041–1061.

Kalnay, E., and Coauthors, 1996: The NCEP/NCAR 40-Year Reanalysis Project. *Bull. Amer. Meteor. Soc.,* **77,** 437–471.

Kanamitsu, M., W. Ebisuzaki, J. Woolen, J. Potter, and M. Fiorino, 1999: An overview of reanalysis-2. *Proc. Second WCRP Int. Conf. on Reanalyses,* WCRP Series Rep. 109, WMO/TD 985, Reading, United Kingdom, WCRP, 1–4.

Kistler, R., and Coauthors, 2001: The NCEP–NCAR 50-year reanalysis: Monthly means CD-ROM and documentation. *Bull. Amer. Meteor. Soc.,* **82,** 247–267.

Lambert, S. J., 1996: Intense extratropical northern hemisphere winter cyclone events: 1899–1991. *J. Geophys. Res.,* **101,** 21 319–21 326.

Lund, R., and J. Reeves, 2002: Detection of undocumented changepoints: A revision of the two-phase regression model. *J. Climate,* **15,** 2547–2554.

Murray, R. J., and I. Simmonds, 1991: A numerical scheme for tracking cyclone centers from digital data. Part I: Development and operation of the scheme. *Aust. Meteor. Mag.,* **39,** 155–166.

Paciorek, C. J., J. S. Risbey, V. Ventura, and R. D. Rosen, 2002: Multiple indices of Northern Hemisphere cyclone activity, winters 1949–99. *J. Climate,* **15,** 1573–1590.

Pettersen, S., 1956: *Weather Analysis and Forecasting.* 2d ed. Vol. 1, McGraw-Hill, 422 pp.

Schubert, S. D., R. B. Rood, and J. Pfaendtner, 1993: An assimilated dataset for earth science applications. *Bull. Amer. Meteor. Soc.,* **74,** 2331–2342.

Serreze, M. C., 1995: Climatological aspects of cyclone development and decay in the Arctic. *Atmos.–Ocean,* **33,** 1–23.

——, F. Carse, R. G. Barry, and J. C. Rogers, 1997: Icelandic low cyclone activity: Climatological features, linkages with the NAO, and relationships with recent changes in the Northern Hemisphere circulation. *J. Climate,* **10,** 453–464.

Simmonds, I., and R. J. Murray, 1999: Southern extratropical cyclone behavior in ECMWF analyses during the FROST Special Observing Periods. *Wea. Forecasting,* **14,** 878–891.

——, and K. Keay, 2000: Variability of Southern Hemisphere extratropical cyclone behavior, 1958–97. *J. Climate,* **13,** 550–561.

——, R. J. Murray, and R. M. Leighton, 1999: A refinement of cyclone tracking methods with data from FROST. *Aust. Meteor. Mag.,* **28,** 617–622.

Sinclair, M. R., 1994: An objective cyclones climatology for the Southern Hemisphere. *Mon. Wea. Rev.,* **122,** 2239–2256.

——, 1997: Objective identification of cyclones and their circulation intensity, and climatology. *Wea. Forecasting,* **12,** 595–612.

Taylor, K., 1986: An analysis of the biases in traditional cyclone frequency maps. *Mon. Wea. Rev.,* **114,** 1481–1490.

Trenberth, K. E., D. P. Stepaniak, and L. Smith, 2005: Interannual variability of patterns of atmospheric mass distribution. *J. Climate,* **18,** 2812–2825.

Uppala, S. M., 2001: ECMWF Reanalysis, 1957–2001. *Proc. ECMWF Workshop on Reanalysis,* ERA-40 Project Rep. Series 3, Reading, United Kingdom, ECMWF, 1–10.

——, and Coauthors, 2005: The ERA-40 re-analysis. *Quart. J. Roy. Meteor. Soc.,* **131,** 2961–3012.

von Storch, H., and F. W. Zwiers, 1999: *Statistical Analysis in Climate Research.* Cambridge University Press, 484 pp.

Wang, X. L., 2003: Comments on "Detection of undocumented changepoints: A revision of the two-phase regression model." *J. Climate,* **16,** 3383–3385.

——, 2006: Climatology and trends in some adverse and fair weather conditions in Canada, 1953–2004. *J. Geophys. Res.,* in press.

——, and Y. Feng, cited 2004: RHTest user manual. [Available online at http://cccma.seos.uvic.ca/ETCCDMI/RHTest/RHTestUserManual.doc.]

——, H. Wan, and V. R. Swail, 2006: Observed changes in cyclone activity in Canada and their relationships to major circulation regimes. *J. Climate,* **19,** 895–916.

Whitaker, L. M., and L. H. Horn, 1984: Northern Hemisphere extra-tropical cyclone activity for four midseason months. *J. Climatol.,* **4,** 297–310.

Woodruff, S. D., R. J. Slutz, R. L. Jenne, and P. M. Steurer, 1987: A Comprehensive Ocean–Atmosphere Data Set. *Bull. Amer. Meteor. Soc.,* **68,** 1239–1250.

Zhang, X., J. E. Walsh, J. Zhang, U. S. Bhatt, and M. Ikeda, 2004: Climatology and interannual variability of Arctic cyclone activity: 1948–2002. *J. Climate,* **17,** 2300–2317.